

Durham Research Online

Deposited in DRO:

06 June 2017

Version of attached file:

Published Version

Peer-review status of attached file:

Peer-reviewed

Citation for published item:

Goes, Saskia and Agrusta, Robert and van Hunen, Jeroen and Garel, Fanny (2017) 'Subduction-transition zone interaction : a review.', *Geosphere.*, 13 (3). pp. 644-664.

Further information on publisher's website:

<https://doi.org/10.1130/GES01476.1>

Publisher's copyright statement:

© The Authors Gold Open Access: This paper is published under the terms of the CC-BY license.

Additional information:

Use policy

The full-text may be used and/or reproduced, and given to third parties in any format or medium, without prior permission or charge, for personal research or study, educational, or not-for-profit purposes provided that:

- a full bibliographic reference is made to the original source
- a [link](#) is made to the metadata record in DRO
- the full-text is not changed in any way

The full-text must not be sold in any format or medium without the formal permission of the copyright holders.

Please consult the [full DRO policy](#) for further details.



Subduction-transition zone interaction: A review

Saskia Goes¹, Roberto Agrusta^{1,2}, Jeroen van Hunen², and Fanny Garel³

¹Department of Earth Science & Engineering, Royal School of Mines, Imperial College, London SW7 2AZ, UK

²Department of Earth Sciences, Durham University, Science Labs, Durham DH1 3LE, UK

³Géosciences Montpellier, Université de Montpellier, Centre national de la recherche scientifique (CNRS), 34095 Montpellier cedex 05, France

ABSTRACT

As subducting plates reach the base of the upper mantle, some appear to flatten and stagnate, while others seemingly go through unimpeded. This variable resistance to slab sinking has been proposed to affect long-term thermal and chemical mantle circulation. A review of observational constraints and dynamic models highlights that neither the increase in viscosity between upper and lower mantle (likely by a factor 20–50) nor the coincident endothermic phase transition in the main mantle silicates (with a likely Clapeyron slope of -1 to -2 MPa/K) suffice to stagnate slabs. However, together the two provide enough resistance to temporarily stagnate subducting plates, if they subduct accompanied by significant trench retreat. Older, stronger plates are more capable of inducing trench retreat, explaining why backarc spreading and flat slabs tend to be associated with old-plate subduction. Slab viscosities that are ~ 2 orders of magnitude higher than background mantle (effective yield stresses of 100–300 MPa) lead to similar styles of deformation as those revealed by seismic tomography and slab earthquakes. None of the current transition-zone slabs seem to have stagnated there more than 60 m.y. Since modeled slab destabilization takes more than 100 m.y., lower-mantle entry is apparently usually triggered (e.g., by changes in plate buoyancy). Many of the complex morphologies of lower-mantle slabs can be the result of sinking and subsequent deformation of originally stagnated slabs, which can retain flat morphologies in the top of the lower mantle, fold as they sink deeper, and eventually form bulky shapes in the deep mantle.

1. INTRODUCTION

The mantle transition zone controls the material and heat exchange between upper and lower mantle. The upper-lower mantle boundary has long been realized to coincide with an endothermic phase transition (Ringwood, 1975; Ito and Yamada, 1982) and to be the likely site of a viscosity increase (Hager, 1984), both of which will hamper flow across the boundary. Mechanisms of Benioff earthquakes and the morphologies of upper-mantle slabs inferred from seismicity and seismic tomography provide direct evidence that the transition zone indeed hinders flow, because many slabs are deformed, and several flattened at the base of the upper mantle (e.g., Lay, 1994; Li et al., 2008). It has been debated (1) what causes some slabs to flatten while others

do not; (2) on what time scales slabs are stagnant in the transition zone if they have flattened; (3) how slab-transition zone interaction is reflected in plate motions; and (4) how lower-mantle fast seismic anomalies can be correlated with past subduction.

Over the past 20 years since the last Subduction Top to Bottom volume and several reviews of subduction through the transition zone (Lay, 1994; Christensen, 2001; King, 2001; Billen, 2008; Fukao et al., 2009), information about the nature of the transition zone and our understanding of how slabs dynamically interact with it has increased substantially. In this review, we will show how, when evaluated together, this past work allows answering the questions above as well as narrowing the plausible properties of the transition zone and slabs. These insights can help the next generation of global-evolution models of mantle convection and can aid further unravelling of what factors may have been responsible for changes in plate motions, plate boundaries, and surface tectonics in the past.

In the first part of the paper (Section 2), we review observational constraints on slab morphology from seismic tomography and slab seismicity, and constraints on subduction dynamics from the plate motion record. Subsequently, in Section 3, we discuss what has been learned from modeling slab dynamics in the transition zone. Figure 1 summarizes the main forces that affect this interaction. Section 3.1 discusses the role of mantle resistance, i.e., the viscosity jump, phase changes, and a potential density jump between the upper and lower mantle; while Section 3.2 covers the role of slab properties, i.e., density and strength, and the mobility of the trench. Finally, in Section 4, we combine the observations with the modeling insights to answer the questions posed above.

2. OBSERVATIONS ON SUBDUCTION-TRANSITION ZONE INTERACTION

2.1. Seismic Imaging: Transition-Zone Slabs

The most detailed information on the structure of slabs as they interact with the transition zone has been obtained from seismic tomography. Before tomographic inversions, Benioff seismicity (Isacks and Molnar, 1971) and analyses of slab structure, for example using the residual sphere technique (Lay, 1994), already indicated that there are different styles of subduction-transition

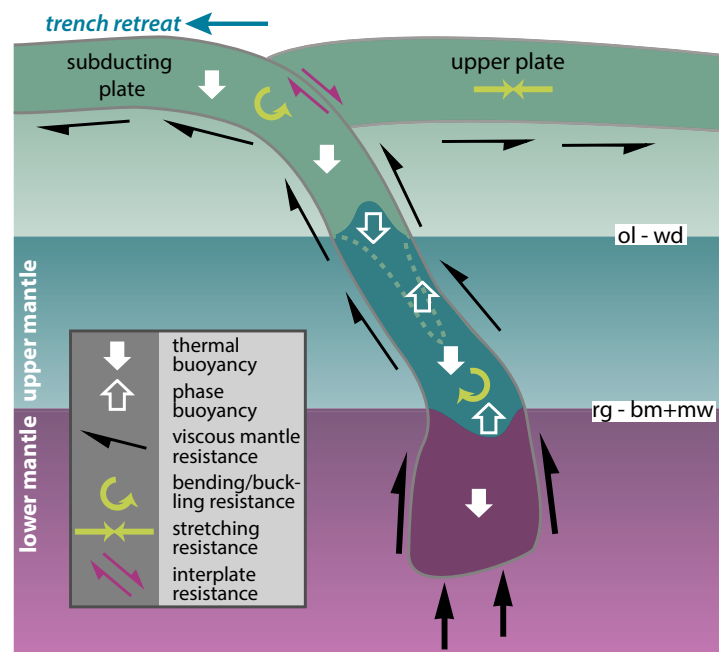


Figure 1. Schematic diagram showing the main forces that affect how slabs interact with the transition zone. The slab sinks driven by its negative thermal buoyancy (white filled arrows). Sinking is resisted by viscous drag in the mantle (black arrows) and the frictional/viscous coupling between the subducting and upper plate (pink arrows). To be able to sink, the slab must bend at the trench. This bending is resisted by slab strength (curved green arrow). The amount the slab needs to bend depends on whether the trench is able to retreat, a process driven by the downward force of the slab and resisted (double green arrow) by upper-plate strength and mantle drag (black arrows) below the upper plate. At the transition from ringwoodite to the postspinel phases of bridgmanite and magnesio-wüstite (rg – bm + mw), which marks the interface between the upper and lower mantle, the slab's further sinking is hampered by increased viscous resistance (thick black arrows) as well as the deepening of the endothermic phase transition in the cold slab, which adds positive buoyancy (open white arrow) to the slab. By contrast, the shallowing of exothermic phase transition from olivine to wadsleyite (ol-wd) adds an additional driving force (downward open white arrow), unless it is kinetically delayed in the cold core of the slab (dashed green line), in which case it diminishes the driving force. Phase transitions in the crustal part of the slab (not shown) will additionally affect slab buoyancy. Buckling of the slab in response to the increased sinking resistance at the upper-lower mantle boundary is again resisted by slab strength.

zone interaction. The first tomographic studies mapped the structure of slabs subducting below the western Pacific, along the Japan-Kurile and Izu-Bonin-Mariana trench (Zhou and Clayton, 1990; Van der Hilst et al., 1991; Fukao et al., 1992) and revealed that some slabs flatten at the base of the transition zone (Izu-Bonin and Japan-southern Kurile), while others appear to pierce straight through to larger depths (Marianas and northern Kurile).

Several generations of tomographic models later, the structure of most subducting slabs in the upper mantle and transition zone has been mapped.

In Figure 2, we compiled the range of slab morphologies in the transition zone from a wide range of tomographic studies (references used are numbered and listed in the caption). Most of the studies we used consist of tomographic inversions of P-wave travel times (using direct as well as surface- or core-bounced phases); a few used S-wave travel times. The studies differ in their data selection and parametrization and regularization of the inversion. Nonetheless, they agree on many aspects of transition-zone slab morphology, which is what we try to capture by our compilation. In the few cases where studies significantly disagree on the interpretation of slab extension or continuity (e.g., below Tonga-Kermadec and North America) or resolution is very limited (e.g., below the Scotia plate), parts of the slab shapes are shaded light blue. To aid discussion of slab volumes and time scales below, the slabs are labeled with the approximate length of the flat segments perpendicular to the present-day trench (in white) or with the approximate depth to which lower-mantle slabs are continuous with those in the upper mantle (in black).

Stagnant slabs are prevalent under the western Pacific, including, besides those listed above, the Ryukyu, Aleutian, and Tonga slabs. Those that do penetrate into the lower mantle below the northwest Pacific are generally not continuous below ~1000 km depth, although there are also significant volumes of fast anomalies deeper in the lower mantle below the region (Van der Hilst et al., 1997; Grand, 2002; Simmons et al., 2012). Lower-mantle anomalies below Tonga and Kermadec extend from ~700 km down to at least 1700 km, but it is not clear whether they are connected to upper-mantle slabs (Van der Hilst, 1995; Schellart and Spakman, 2012).

The classic example of a deeply penetrating plate is the Cocos plate, subducting along the eastern side of the Pacific, below Central America (Grand et al., 1997). However, this is clear only along a few cross sections through a rather complex slab, which changes its strike from more or less west-east in the upper mantle below Mexico, parallel to the Trans-Mexican Volcanic Belt, to more or less north-south in the lower mantle below the Gulf of Mexico and the United States (Gorbatov and Fukao, 2005). Along other profiles below the Americas, significant thickening is observed in the transition-zone slab below Peru, where it penetrates the lower mantle down to only ~1500 km depth, while slab flattening appears to occur in the transition zone below Cascadia, Mexico and southern South America (Sigloch et al., 2008; Simmons et al., 2012; Fukao and Obayashi, 2013). Slab fragments that lie in the transition zone below the United States are generally associated with previous (Laramide) subduction (Van der Lee and Nolet, 1997; Sigloch, 2011), and their connection to the prominent lower-mantle anomaly below eastern North America is debated (Bunge and Grand, 2000; Schmid et al., 2002; Ren et al., 2007; Sigloch and Mihalynuk, 2013).

Fukao and coworkers (Fukao et al., 2001; Fukao et al., 2009; Fukao and Obayashi, 2013) proposed that there is a significant amount of material trapped below 660 km and above 1000 km depth, in particular below Indonesia, Tonga-Kermadec, and South America. In tomographic models from other groups, there is little evidence of ponding above 1000 km, apart from the material below Borneo, Indonesia, which is found in many studies (Hafkenscheid

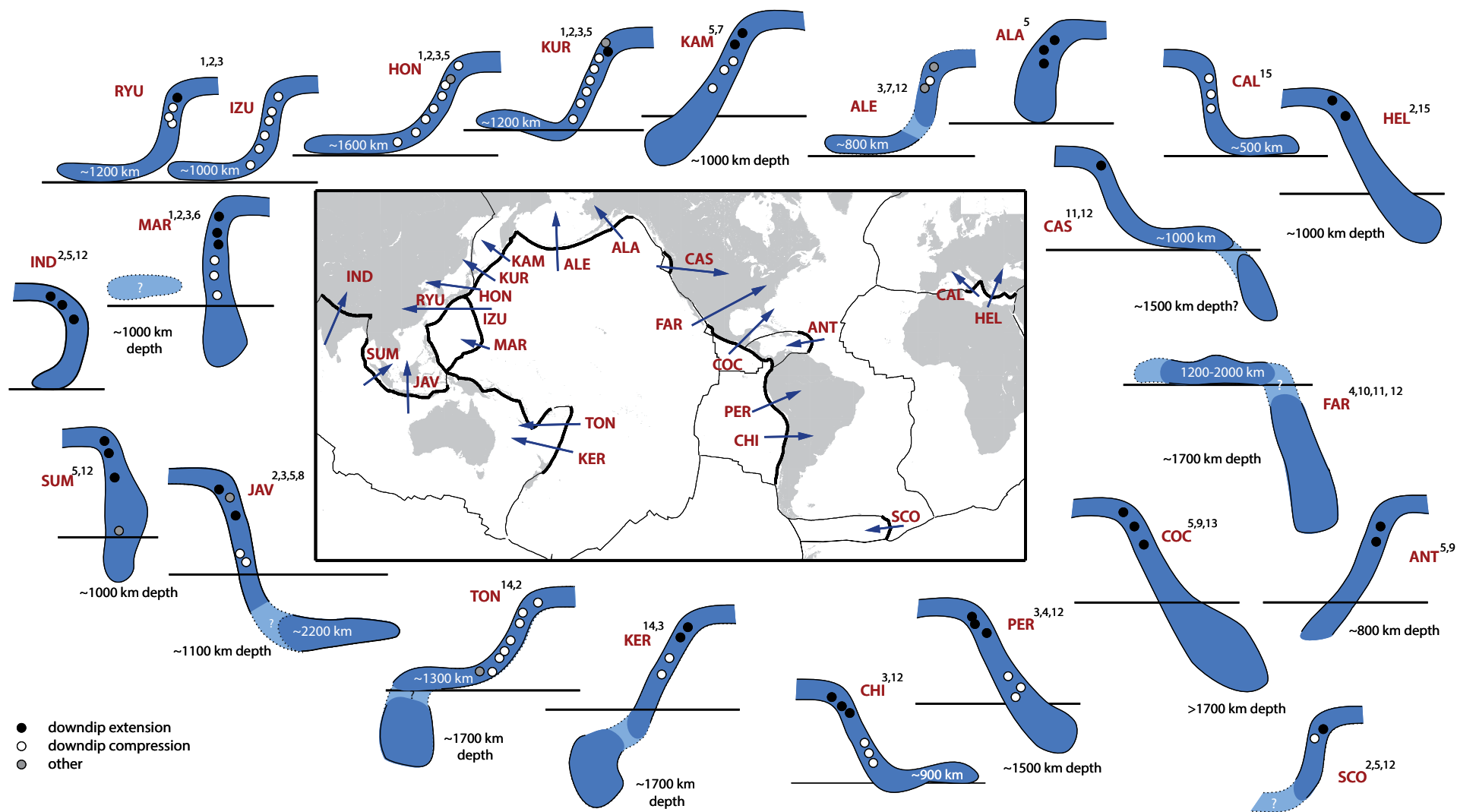


Figure 2. Summary of morphologies of transition-zone slabs as imaged by tomographic studies and their Benioff stress state. Arrows on the map indicate the approximate locations of the cross sections shown around the map, with their points in down-dip direction. Blue shapes are schematic representations of slab morphologies (based on the extent of fast seismic anomalies that were tomographically resolvable from the references listed). Horizontal black lines indicate the base of the transition zone (~660 km depth). For flattened slabs, the approximate length of the flat section is given in white text inside the shapes. For penetrating slabs, the approximate depth to which the slabs are continuous is given in black text next to the slabs. Circles inside the slabs indicate whether the mechanisms of earthquakes at intermediate (100–350 km) and deep (350–700 km) are predominantly down-dip extensional (black) or compressional (white). Stress states are from the compilations of Isacks and Molnar (1971), Alpert et al. (2010), Bailey et al. (2012), complemented by Gorbato et al. (1997) for Kamchatka, Stein et al. (1982) for the Antilles, McCrory et al. (2012) for Cascadia, Papazachos et al. (2000) for the Hellenic zone, and Forsyth (1975) for Scotia. The subduction zones considered are (from left to right and top to bottom): RYU—Ryukyu, IZU—Izu, HON—Honshu, KUR—Kuriles, KAM—Kamchatka, ALE—Aleutians, ALA—Alaska, CAL—Calabria, HEL—Hellenic, IND—India, MAR—Marianas, CAS—Cascadia, FAR—Farallon, SUM—Sumatra, JAV—Java, COC—Cocos, ANT—Antilles, TON—Tonga, KER—Kermadec, CHI—Chile, PER—Peru, SCO—Scotia. Numbers next to the red subduction zone codes refer to the tomographic studies used to define the slab shapes: 1—Van der Hilst et al., 1991; Fukao et al., 1992; 2—Bijwaard et al., 1998; Hafkenscheid et al., 2001; Hafkenscheid et al., 2006; 3—Fukao et al., 2001; Fukao et al., 2009; Fukao and Obayashi, 2013; 4—Bunge and Grand, 2000; Grand, 2002; 5—Karason and Van der Hilst, 2000; Replumaz et al., 2004; Li et al., 2008; 6—Miller et al., 2005; Miller et al., 2006; 7—Gorbato et al., 2000; 8—Hall and Spakman, 2015; 9—Van der Hilst, 1989; Grand et al., 1997; Ren et al., 2007; 10—Van der Lee and Nolet, 1997; Schmid et al., 2002; 11—Sigloch et al., 2008; Sigloch, 2011; 12—Simmons et al., 2012; 13—Gorbato et al. and Fukao, 2005; 14—Van der Hilst, 1995; Schellart and Spakman, 2012; 15—Spakman et al., 1993; Wortel and Spakman, 2000; Piromallo and Morelli, 2003.

et al., 2001; Replumaz et al., 2004; Simmons et al., 2012). The recent *P*-velocity model of Simmons et al. (2012) instead finds even more extensive amounts of material sequestered above 660 km, including below Kamchatka and Hellenic arc, where most previous studies have suggested the slabs penetrate. Some of the slabs (e.g., below South America) may appear flat when cross sections are taken obliquely through relatively complex slab geometries. For Kermadec, the interpretations of the lower-mantle anomalies range from flattened (Fukao and Obayashi, 2013) to just thickened (Schellart and Spakman, 2012). French and Romanowicz (2014) note that their recent global shear-speed model confirms the flattened slab material that Fukao et al. (2009) identified in the uppermost lower mantle. However, they only show a cross section for Kermadec, which could be interpreted as either flattening over ~500 km below 660 km or thickening. Rather than being flat, the Indonesia deep flat slab has been suggested to represent a cluster of slab material subducted at different zones and not connected directly to the steep upper slab below Java (Hall and Spakman, 2015). Thus it appears that very few, if any, slabs actually flatten below 700 km depth.

A few previous studies (Loiselet et al., 2010; King et al., 2015) have noted a broad correlation between stagnant slabs and their estimated thermal structure (based on the age of the subducting plate and its subduction velocity). Indeed, stagnant slabs are common in the western Pacific, where very old lithosphere is currently subducting (90–145 m.y., Müller et al., 2008), while some deeply penetrating slab sections are found along the eastern rim of the Pacific, where the lithosphere currently subducting is relatively young (0–50 m.y., Müller et al., 2008). In more detail, there may be further complexity. For example, the penetrating segment of the Izu-Bonin-Marianas slab corresponds to the oldest lithosphere along this trench, while at the Tonga-Kermadec and the Japan-Kuriles-Kamchatka trenches, the youngest part of the lithosphere penetrates. However, all lithosphere currently subducting along these trenches has an age (>90 m.y.) that exceeds that above which plates appear to no longer thicken and increase their negative buoyancy (Stein and Stein, 1992; Davaille and Jaupart, 1994). Additionally, it has long been observed that there is no simple correlation between present-day slab dip and age at the trench (Lallemand et al., 2005; Sdrolias and Müller, 2006). Along each trench there has been a large variation in age of the subducting plate during the Cenozoic, which may be one reason that there are no simple correlations with slab geometry (e.g., Garel et al., 2014).

Also noted (in white text) on Figure 2 are the approximate lengths of the flat slabs in the transition zone. These range from several hundred km (below Calabria) to up to 2000 km (below North America and, if this is indeed a flat slab, below Borneo). At subduction rates of 5 cm/yr (i.e., around the global average; Lallemand et al., 2005; Sdrolias and Müller, 2006), and without significant stretching or thickening, 1000 km corresponds to ~20 m.y. of subduction. Comparison of tomography with plate reconstructions has led to estimates of accumulation times, i.e., stagnation times, around such a number, e.g., for the ~1000-km-long, flat Izu-Bonin slab, 20–30 m.y. (Van der Hilst and Seno, 1993; Miller et al., 2006; Sdrolias and Müller, 2006); for the ~1600 km Honshu flat

slab, more than 15–20 m.y. (Miller et al., 2006; Goes et al., 2008); for the Tonga flat segment of ~1300 km, ~30–40 m.y. (Van der Hilst, 1995; Sdrolias and Müller, 2006; Schellart and Spakman, 2012); and for the ~500-km-long, Calabrian flat slab, 8–10 m.y. (Wortel and Spakman, 2000; Faccenna et al., 2001). Schmid et al. (2002) estimated that the Farallon material in the transition zone corresponds (due to buckling) to subduction since 50–60 m.y. ago. The deeper flat slab below Indonesia has been associated with opening of the South China Sea 30–40 m.y. ago (Replumaz et al., 2004). These numbers imply that material can indeed stagnate in the transition zone for a few tens of millions of years. However, there is no seismic evidence of older material in the upper mantle and transition zone. Because the time scales to diffuse the thermal anomaly of a cold slab and hence make it seismically invisible are on the order of hundreds of millions of years, material subducted in the early Cenozoic and Mesozoic has apparently sunk into the deeper mantle.

2.2. Wadati-Benioff Seismicity

Focal mechanisms provided the earliest evidence that slabs encounter resistance as they reach the base of the upper mantle. Most slabs exhibit either down-dip extension or compression, where globally, extension is most common above 300–350 km depth, while below this depth all slabs that exhibit deep seismicity are dominantly under compression (Isacks and Molnar, 1971; Apperson and Frohlich, 1987; Alpert et al., 2010). Richter (1979) showed that, in addition to increasing down-dip compression in earthquake mechanisms, there is a bulge in seismic energy release above the base of the upper mantle, between 500 and 700 km depth, which can be reconciled with increased resistance at this depth. Initially, it was thought that these observations and the absence of seismicity below 700 km depth meant slabs stopped at this depth, until several studies established that the depth extent of seismicity is linked to how deep the slab core remains cooler than a potential temperature of 600–800 °C (Molnar et al., 1979; Wortel, 1982), and studies of seismic structure showed that many slabs extend beyond their Benioff zones (e.g., Van der Hilst et al., 1991; Fukao et al., 1992; Lay, 1994; Grand et al., 1997).

Vassiliou and Hager (1988) showed that earthquake stress directions could be matched with models of viscous sinking slabs encountering a viscosity increase of, at least, an order of magnitude at 660 km depth, the mechanism previously proposed by Isacks and Molnar (1971). More recent studies (Alpert et al., 2010; Bailey et al., 2012), using global-flow models driven by plate motions and slabs with viscosities 1–2 orders of magnitude higher than the background upper mantle that track the Benioff zones, can match the global pattern of down-dip slab extension and compression with an upper-lower mantle viscosity jump of 30–100.

There is regional variation on the global pattern: while most slabs exhibit extension at intermediate depths (100–350 km), some, in particular in the western Pacific, are compressional throughout their depth range (including Japan, Kurile, Izu-Bonin, and Tonga; see Fig. 2) (Isacks and Molnar, 1971). A

few studies have modeled the difference in stress patterns as the result of a net westward rotation of the lithosphere relative to the lower mantle, which enhances compression in westward-dipping slabs and extension in eastward-dipping ones (Alpert et al., 2010; Carminati and Petricca, 2010). However, another study was able to match the difference in Benioff stress patterns in the Tonga and South American slabs in a global mantle flow model as a result of differences in slab geometry (Alisic et al., 2010). Earlier studies (Isacks and Molnar, 1971; Vassiliou and Hager, 1988) had proposed instead that the slabs with compression throughout were more supported by the lower mantle than those with intermediate depth extension. The compilation in Figure 2 provides support for the earlier interpretation because (1) not all westward-dipping slabs are in compression throughout (e.g., Marianas and Kermadec), and not all eastward-dipping slabs exhibit intermediate depth extension (e.g., Calabria); and (2) the slabs with compression throughout tend to be those that flatten in the transition zone (with the exception of the Chilean slab). This includes slabs that are too warm to sustain deep seismicity, such as the Aleutian, Ryukyu, and Scotia flattened slabs, where the former two have previously been identified as outliers of the usual trend of downdip extension in slabs without Benioff seismicity below 350 km (Isacks and Molnar, 1971; Bailey et al., 2012).

Others have used seismicity to estimate the amount of deformation that occurs in upper-mantle slabs, a measure that can be used as a constraint on slab strength. Already from Benioff-zone geometries, it is clear that there is slab bending and contorting (e.g., Alpert et al., 2010; Hayes et al., 2012). Moment tensors provide further evidence of bending, folding, and shearing on top of the overall downdip stress patterns (Giardini and Woodhouse, 1984; Apperson and Frohlich, 1987; Bailey et al., 2012; Myhill, 2012). Moment tensor summations for the seismicity in the Tonga slab (by far the most seismically active Benioff zone) show that ~50% of the sinking is accommodated by internal deformation (Fischer and Jordan, 1991; Holt, 1995), implying effective upper-mantle slab viscosities of no more than 2 orders of magnitude higher than the surrounding mantle (e.g., review by King, 2001; Alisic et al., 2010).

2.3. Seismic Tomography: Lower-Mantle Slabs

Lower-mantle seismic anomalies that are attributed to past subduction come in a wide range of shapes, from relatively linear and dipping (Farallon under Central America, northern Kurile, Aegean), to vertical and short (Marianas), flattened in top of lower mantle (Java-Borneo) to broad anomalies that do not have a slab shape, e.g., below the Indian plate and in the deepest mantle around the Pacific (Karason and Van der Hilst, 2000; Grand, 2002; Hafkenscheid et al., 2006). Many studies have concluded that the lower-mantle anomalies correspond to thicker volumes of material than the upper-mantle slabs, even considering limitations of seismic resolution. Several studies have estimated that some slabs, e.g., the Cocos, Java, and Hellenic slabs, thicken by a factor of 4–5 upon entering into the lower mantle, to widths of ~400 km (Ribe et al., 2007; Loiselet et al., 2010), or even 400–700 km for the slabs below North

America (Sigloch and Mihalynuk, 2013); while thickening in the lower-mantle slab anomalies below the Indian plate has been estimated to be about a factor of 3 (Hafkenscheid et al., 2006). Such strong thickening has commonly been attributed to slab buckling that starts in the transition zone (Ribe et al., 2007; Běhounková and Čížková, 2008; Lee and King, 2011). Thickening has been inferred to be less for some of the older penetrating slabs below the western Pacific (Marianas, Kermadec, Loiselet et al., 2010) but may still be a factor of two, an amount which can also be achieved by simple compressional thickening (Gurnis and Hager, 1988; Běhounková and Čížková, 2008).

At mid-mantle depths, there are two prominent belts of high-velocity anomalies (Van der Hilst et al., 1997; Bijwaard et al., 1998; Grand, 2002). One stretches below the Americas from the northern tip of Canada to Bolivia and is generally attributed to Farallon subduction (Grand, 1994; Van der Hilst et al., 1997; Bunge and Grand, 2000; Ren et al., 2007), although recently an interpretation involving additional oceanic plates has been advanced (Sigloch and Mihalynuk, 2013). The other anomaly more or less underlies the Tethyan suture zone stretching from the Aegean to Indonesia (Van der Hilst et al., 1997; Van der Voo et al., 1999b). These Tethys- and Farallon-attributed anomalies extend to depths from 700 to 1000 km down to 1700–2000 km depth (Van der Hilst et al., 1997; Bijwaard et al., 1998; Grand, 2002). Each of these belts is made up of a number of segments, and within the Tethyan anomalies several parallel belts, attributed to separate subduction zones, have been identified (Van der Voo et al., 1999b; Hafkenscheid et al., 2006; Nerlich et al., 2016). By comparing these anomalies with plate reconstructions, they have been estimated to represent subduction of the past 100–140 m.y. (Grand, 1994; Hafkenscheid et al., 2006; Sigloch and Mihalynuk, 2013). These ages imply lower-mantle slab sinking rates of 1–2 cm/yr (Grand, 1994; Hafkenscheid et al., 2006; Van der Meer et al., 2009; Sigloch and Mihalynuk, 2013; Butterworth et al., 2014; Domeier et al., 2016). Deeper anomalies may correspond to subduction going back as far as 200 m.y. ago and in a few locations even 300 m.y. (Richards and Engebretson, 1992; Ricard et al., 1993; Van der Voo et al., 1999a; Van der Meer et al., 2009), although it has been questioned how robust correlations between plate-motion history and anomalies below 2300 km depth are (Domeier et al., 2016).

As discussed above, slabs appear to thicken as they transit from the upper to the lower mantle. A further change in morphology occurs toward the deep mantle, where bulky fast regions rather than linear belts of anomalies are found. High-velocity anomalies in the deepest 500 km of the mantle more or less encircle the Pacific with a particularly large pond of fast material below eastern Asia, as well as others below the Americas and the southern Indian Ocean (Van der Hilst et al., 1997; Grand, 2002; Simmons et al., 2012). These changes in morphology with depth have been suggested to be a simple consequence of slab deformation during sinking (Grand, 2002; Jarvis and Lowman, 2007).

In sum, the tomographic evidence shows that slabs experience significant resistance at the base of the transition zone leading to flattening, buckling, and thickening, and further deformation to less linear forms on their journey

through the lower mantle. Comparisons with plate reconstructions constrain the time scales of slab sinking into the lower mantle to 10–50 m.y. and through the rest of the mantle to 150–200 m.y. Even if many subduction zones have been long lived (e.g., along the circum-Pacific), the slabs are generally not continuous over the full mantle depth range, indicating that the sinking process is discontinuous, as previously noted by Grand (2002), which may reflect the influence of stagnation in the transition zone.

2.4. Plate Motions

Most Cenozoic downgoing plate motions range between ~5 and 10 cm/yr (Sdrolias and Müller, 2006; Müller et al., 2008; Goes et al., 2011; Zahirovic et al., 2015), and there is a correlation of increasing velocity with the age of the plate at the trench (Carlson et al., 1983; Lallemand et al., 2005; Goes et al., 2011). This range and the age trend have been interpreted as an expression of upper-mantle slab pull as driving force of the plates (Conrad and Lithgow-Bertelloni, 2002; Faccenna et al., 2007; Goes et al., 2011). Some segments of the Farallon plate moved notably faster (≥ 15 cm/yr) (Müller et al., 2008), as did the Indian plate before 50 m.y. ago (Lee and Lawver, 1995; Müller et al., 2008; Capitanio et al., 2010a). It has been suggested that these fast motions are due to: plate avalanching into the lower mantle (Goes et al., 2008), to the setting up of a whole mantle convection circulation, as opposed to upper-mantle confined cells (Becker and Faccenna, 2011; Faccenna et al., 2013), and for India, the push of the Reunion plume and consequent lowering of asthenospheric viscosities below the plate (Cande and Stegman, 2011; van Hinsbergen et al., 2011), a pull by double subduction (Jagoutz et al., 2015) or the removal of the Indian cratonic keel (Kumar et al., 2007), or the interplay of several of these factors (Zahirovic et al., 2015).

The large majority of trenches (~70% of the segments throughout the Cenozoic) retreat (Sdrolias and Müller, 2006; Müller et al., 2008; Schellart et al., 2008; Goes et al., 2011; Williams et al., 2015). This is true irrespective of the hotspot reference frame used, but an Indo-Atlantic or global hotspot reference frame is most consistent with slab shapes and dynamic considerations (Schellart et al., 2008; Goes et al., 2011; Williams et al., 2015). Most trench motions are between ~1 cm/yr (advancing) and +2 cm/yr (retreating) (Williams et al., 2015), and, on average, trench retreat accounts for ~10% of the convergence velocities (Goes et al., 2011). Some trenches retreated significantly faster (motions up to 10 cm/yr) during part of the Cenozoic (Tonga, Izu-Bonin, Japan, and Calabria). A few trenches advance(d) (Marianas and Kermadec since ~10 m.y. ago, and the Sumatran end of the Sunda trench and Alaskan end of the Aleutian trench at slow rates, <1 cm/yr). Throughout the Cenozoic, trench motions that exceed 1–2 cm/yr (both in advance and retreat) are only observed for older plates (>50 m.y.) (Fig. 3; Molnar and Atwater, 1978; Sdrolias and Müller, 2006; Goes et al., 2011).

It has been noted that although there is some correlation between absolute downgoing-plate motions and age, there is no correlation between present-day

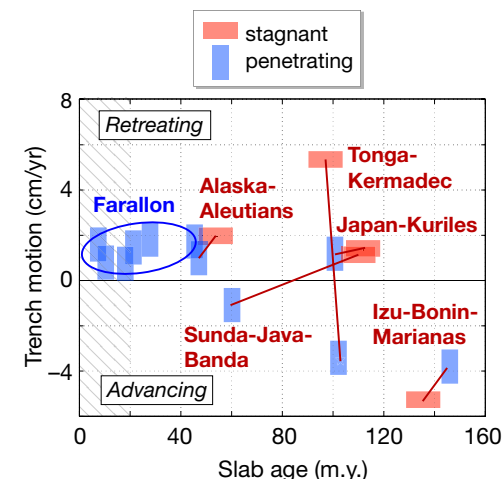


Figure 3. Present-day trench motion versus plate age at the trench for a selection of subduction zones. There is no simple relation between slab behavior in the transition zone and either plate age at the trench or trench motion at the present day (data from Sdrolias and Müller, 2006). Red lines connect points along the same trench.

trench motions and slab morphology or dip (King, 2001; Lallemand et al., 2005; Billen, 2008; Fig. 3). On the other hand, it is also well established that there is a correlation between trench-motion history and plate morphology (e.g., Van der Hilst and Seno, 1993; Faccenna et al., 2001) (Fig. 4). In Figure 4, we compiled estimates of the total trench retreat (references in the caption), measured approximately perpendicular to the present-day trench during the past 50 m.y. Uncertainties in the measurements are probably $\sim \pm 200$ km, due to uncertainties in the reconstructions and reference frame. It should be noted that the total trench motions were generally achieved in only part of these 50 m.y. (Clark et al., 2008), e.g., for Tonga during the past 35 m.y. in two phases (Sdrolias and Müller, 2006), for Scotia during the past 40 m.y. during several phases (Barker, 2001), for Calabria during the past 15 m.y. (Faccenna et al., 2001), and corresponded to trench velocities from 2 to ~10 cm/yr. Most flattened slabs seem to have undergone trench retreat at a rate of at least 2 cm/yr at some point in their Cenozoic history (Sdrolias and Müller, 2006). When integrated over the past 50 m.y., all trenches, except India, which advanced by ~1500 km (Replumaz et al., 2004; Hafkenscheid et al., 2006) (not included in Fig. 4), show a net retreat, over distances ranging from a few hundred km to 2000 km.

The history of trench retreat generally correlates with the morphology of the slab in the transition zone (Fig. 4). The Indian slab (not shown) is the only one that is rolled over and the only one that underwent a net trench advance. All other slabs are reclining, as expected from a net trench retreat. Most slabs that penetrate into the lower mantle subducted at relatively stable trenches,

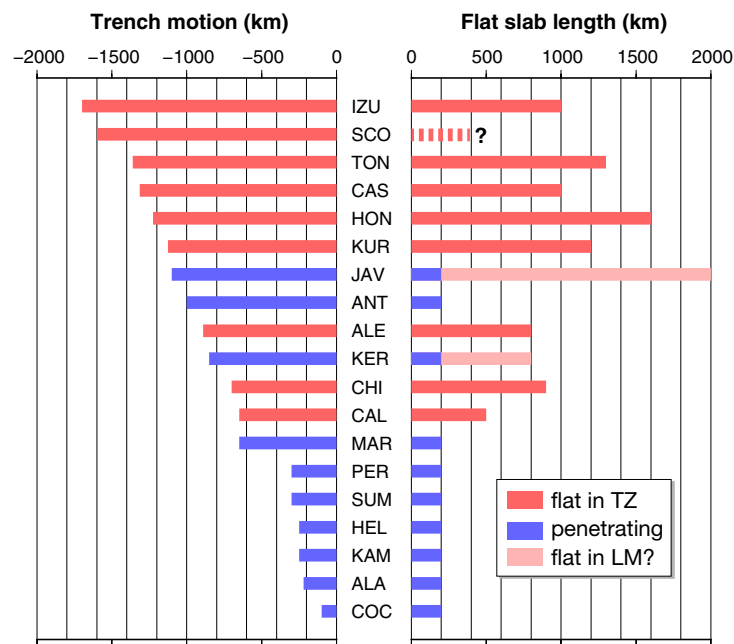


Figure 4. Estimates of total trench retreat over the past ~50 m.y. compared with the estimates of flat-slab length from Figure 2. Distances of trench retreat approximately perpendicular to the trench have been compiled from Ross and Scotese (1988), Jolivet and Faccenna (2000), Barker (2001), Faccenna et al. (2001), Schellart et al. (2003), Replumaz et al. (2004), Miller et al. (2006), Sdrolias and Müller (2006), Ren et al. (2007), Müller et al. (2008), and Schellart and Spakman (2012). For penetrating slabs, a thickness of 200 km is assigned because all of them thicken as they enter the lower mantle (LM). For the Scotia flat slab, no length can be estimated. Bright red bars are for slabs that flatten in the transition zone (TZ); light red bars for those that have been proposed to flatten below 700 km depth. Blue bars are for slabs that penetrate into the lower mantle. Flat-slab lengths and abbreviations as in Figure 2.

while flat slabs all have a history of significant trench retreat (>800 km). For example, along the Tonga-Kermadec, Izu-Bonin-Marianas, Japan-Kurile-Kamchatka trenches, the penetrating parts of the slab subducted where the trench moved the least over the past 50 m.y. The trenches bordering the west coast of the Americas overall moved westward by ~1000 km (Grand, 1994; Ren et al., 2007; Müller et al., 2008); however, due to the shape of the trench and relative North and South American motions, trench motion reached a minimum near Peru and was almost zero off Central America, the only place where a slab appears to penetrate directly and deeply into the lower mantle.

For a few of the penetrating slabs, under the Antilles, Java, and Kermadec, the trenches retreated as much as for some of the flat slab cases. The Antilles slab seems to penetrate even though most plate tectonic studies (starting with Ross and Scotese, 1988) have inferred that its trench has undergone >1000 km of retreat. However, some studies have challenged this view and

concluded the trench was formed only ~300 km westward of its current position (James, 2009). It is also possible that interaction with the nearby Cocos plate has played a role in forcing the penetration of the Antillean slab with the transition zone. In several reconstructions (Replumaz et al., 2004; Müller et al., 2008), the Java trench retreated over ~2000 km, largely achieved while the South China Sea opened, and the flat slab segment at ~1100 km depth has been linked to this retreat (Replumaz et al., 2004). On the other hand, a recent study attributed both the extension phase and the (inferred to not be flattened) slab segments in the lower mantle to different subduction systems (Hall and Spakman, 2015). Kermadec is another location where a lower-mantle flat slab segment, of up to ~800 km length, similar to the reconstructed amount of trench retreat, has been suggested (Fukao and Obayashi, 2013), although others interpret the deeper slab structure as thickened rather than flattened (Schellart and Spakman, 2012).

The lengths of the flat slabs are similar (most in the range 800–1600 km) to the estimates of trench retreat (Fig. 4), where it should be borne in mind that uncertainties in flat-slab length are likely larger than those in the trench motion estimates, due to variable seismic resolution and subjectivity in defining the extent of the slab.

3. MODELS OF SUBDUCTION-TRANSITION ZONE DYNAMICS

The many modeling studies done, on how slabs interact with the mantle transition zone, show that there are two main sets of factors (Fig. 1) that can affect whether slabs stagnate or penetrate: (1) the mantle resistance to flow through the upper-lower mantle boundary; and (2) the shape and strength of the slab as it starts interacting with this boundary, where the ability of the trench to retreat plays a crucial role in the former. We will discuss the relative importance of each of these below.

3.1. Role of Mantle Resistance

Several factors have been proposed to contribute to the resistance to sinking at the base of the upper mantle, most prominently a jump in viscosity between upper and lower mantle (Section 3.1.1) and the deflection of the endothermic phase transition from ringwoodite to the postspinel phases bridgmanite and magnesiowüstite in the cold slab, which locally reduces the slab's negative buoyancy (Section 3.1.2). Some studies have suggested that additionally a (small) change in intrinsic density due to variations in chemistry between upper and lower mantle may contribute (Section 3.1.3).

3.1.1. Viscosity Jump

Modeling of the geoid, postglacial rebound, free-air gravity, and dynamic topography observations constrains the average viscosity of the lower mantle to be a factor 10–100 higher than the average upper-mantle viscosity (e.g., Chen and King, 1998; Panasyuk and Hager, 2000; Mitrovica and Forte, 2004).

Similar increases in viscosity of the lower relative to the upper mantle have been inferred from models that reproduce lower-mantle slab sinking velocities estimated from the match of plate reconstructions with tomography (Čížková et al., 2012).

Because experiments show that viscosity varies exponentially with pressure (and exponentially with the inverse of temperature), part of this increase may be a gradual pressure effect (in particular in the shallow lower mantle, e.g., Marquardt and Miyagi, 2015; King, 2016), a trend that will, to some extent, be offset by the decrease in viscosity due to adiabatically increasing temperature with depth (Ranalli, 1995; King, 2016). On the other hand, the phase transition in most of the mantle minerals at the base of the upper mantle is a logical place for a step in viscosity to occur (Karato, 1989; Faccenda and Dal Zilio, 2017). Some joint inversions also require a jump close to this depth (Mitrovica and Forte, 2004). Furthermore, experiments show that bridgmanite, which comprises ~80% of the lower-mantle composition, is a relatively strong phase (Yamazaki and Karato, 2001). Additionally, geoid modeling of the signature above subduction zones indicates that the resistive effect of an endothermic phase transition has a low signal and an increase in viscosity at the boundary, by a factor 30–100, is required to explain smaller-scale geoid structure (King, 2002; Tosi et al., 2009), where it should be borne in mind that dynamically, a strong viscosity-depth gradient will have a similar effect as a sharp jump.

Global-scale models of mantle convection find that the range of upper- to lower-mantle viscosity jumps inferred from observations does not lead to layered convection or lead to a significant accumulation of slab material in the transition zone (Van Keken and Zhong, 1999; Yanagisawa et al., 2010). Regional models, of a single subduction system, do generate a range of slab morphol-

ogies in response to such a viscosity increase but only if the trench can move freely (Kincaid and Olson, 1987; Gurnis and Hager, 1988; Guillou-Frottier et al., 1995; Christensen, 1996; Olbertz et al., 1997; Garel et al., 2014). The regional-model slab morphologies resemble the diversity of geometries imaged tomographically (Fig. 5).

However, in models with only a viscosity jump, even if the slabs flatten, lower-mantle sinking velocities are not negligible, and as a result, they are not able to generate flat-slab segments of the >1000 km length inferred from tomographic images (Garel et al., 2014). On the other hand, if there is no viscosity jump, it is difficult to develop any flat slabs (Tagawa et al., 2007; Torii and Yoshioka, 2007; Yanagisawa et al., 2010; and our own models for Fig. 6). At the high end of the geoid and rebound-based viscosity jumps—a factor of 100 or higher—slab sinking into the lower mantle is strongly impeded (Běhouňková and Čížková, 2008; Loiselet et al., 2010), trench retreat decreased (Čížková and Bina, 2013; Garel et al., 2014), and the range of slab morphologies is limited to flattening and folding, even if slab cores are 2–3 orders of magnitude more viscous than the surrounding mantle (Garel et al., 2014).

3.1.2. Endothermic Phase Transition

The downward deflection of the endothermic ringwoodite to bridgmanite + magnesiowüstite transition within the cold slabs leads to a local increase in buoyancy of the slabs, which hampers their further descent (e.g., Bina et al., 2001; Faccenda and Dal Zilio, 2017). In a pyrolitic composition, along a background (1300 °C potential) mantle temperature profile, the density jump at the ringwoodite to postspinel transition is 220 kg/m³ (calculated with the database

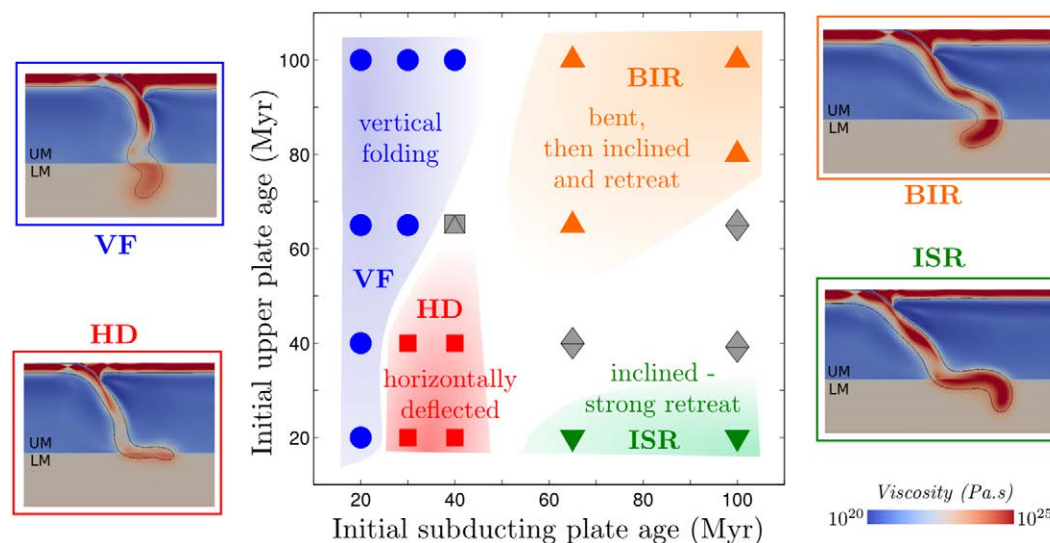


Figure 5. Modified from Garel et al. (2014). With a viscosity jump of a factor of 30 between upper (UM) and lower mantle (LM), different deformation modes (model snap shots on the sides) are possible for subducting and upper plates of different initial ages (central regime diagram), and some slabs may appear stagnant in their upper-mantle morphology (HD and ISR). However, all slabs attain lower-mantle sinking velocities that are 0.5 cm/yr (for the HD cases) or larger.

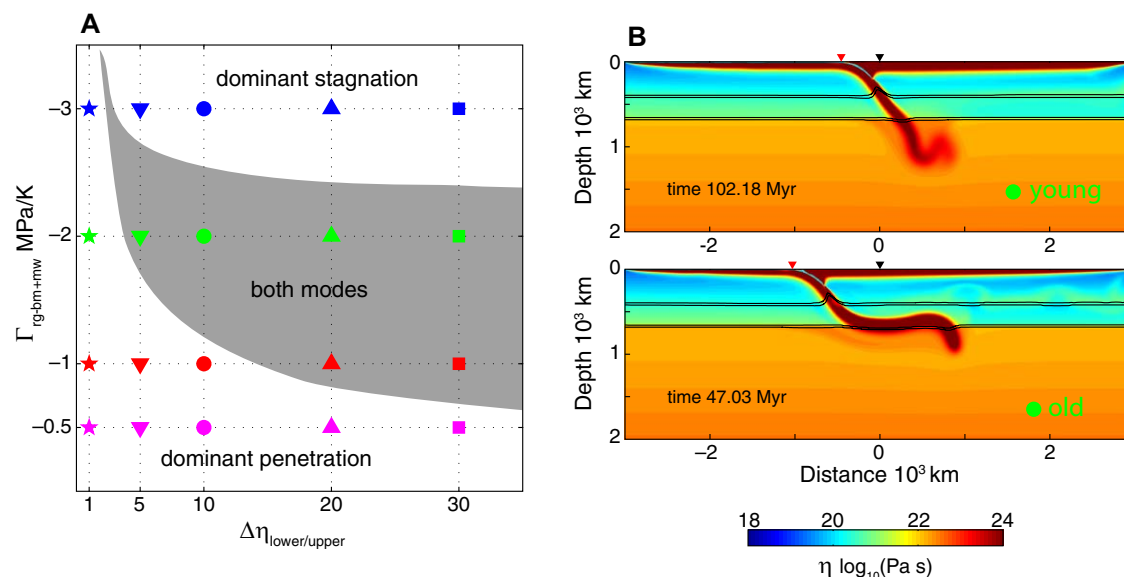


Figure 6. Modified from Agrusta et al. (2017). (A) Regime diagram showing where old and young slabs either both penetrate ("dominant penetration"), both stagnate ("dominant stagnation"), or old ones stagnate while young ones penetrate ("both modes") as a function of upper-lower mantle viscosity jump ($\Delta\eta_{lower/upper}$) and postspinel transition Clapeyron slope ($\Gamma_{rg-bm+mw}$). Without a viscosity jump, no slabs stagnate; but if a jump is included, then the variation in Clapeyron slope is more efficient in stagnating slabs in the transition zone than further variation in the viscosity jump, due to the large density jump associated with the $rg-bm+mw$ phase transition. (B) An example snapshot of slab geometry for old and young slabs for the case marked by a green circle in section A. Colors represent viscosity; and black lines represent the depths at which 1% and 99% of the olivine to wadsleyite (near 400 km depth) and postspinel (near 660 km depth) transitions are complete. Black and red triangles show the initial and current position of the trench, respectively. Because of their higher potential for trench retreat, old plates are more prone to stagnation than young ones.

from Stixrude and Lithgow-Bertelloni, 2011) (a 5.5% density increase relative to the density above the transition). Compared with the excess density of slabs, which ranges from $\sim 30 \text{ kg/m}^3$ for young plates to up to 100 kg/m^3 for very old plates (Cloos, 1993), it is clear that a downward deflection of the transition makes the slabs locally buoyant, thus providing a very strong stagnating force.

The slab's buoyancy due to the deflected phase transition in the downgoing slab is only a localized effect. Once part of the slab manages to sink below the transition, its negative buoyancy is regained. The joint influence of the density jump and phase boundary deflection is described by the phase buoyancy parameter, a measure of the local buoyancy due to the phase transition compared with overall thermal convective driving force (Christensen and Yuen, 1985). The most recent experimental estimates for the Clapeyron slope, Γ , of the ringwoodite to postspinel transition are between -0.5 and -2.0 MPa/K (Hirose, 2002; Fei et al., 2004; Katsura et al., 2004; Litasov et al., 2005; Stixrude and Lithgow-Bertelloni, 2011). At the lowest temperatures (below $900\text{--}1400^\circ\text{C}$ [Stixrude and Lithgow-Bertelloni, 2011; Holland et al., 2013]), the also strongly endothermic transition (Γ between -2 and -5 MPa/K) from ringwoodite through akimotoite to bridgmanite and magnesio-wüstite may further contribute to the slab's phase buoyancy (Faccenda and Dal Zilio, 2017).

Many modeling studies have investigated how slab material may be sequestered in the transition zone by the effect of a negative Clapeyron slope or a combined viscosity jump and Clapeyron slope effect, starting with Richter (1973), who showed that it could somewhat hinder convection. Christensen and Yuen (1984) did a detailed investigation of the interaction of a vertically

sinking slab across a boundary with an endothermic phase change and/or chemical density changes of variable strength. They showed that for very high slopes, more than -4 to -6 MPa/K , the phase buoyancy effect is so strong that convection becomes layered. Many subsequent models have shown that for intermediate Clapeyron slopes, above -2 to -3 MPa/K (i.e., at the high end of current experimental constraints), partial layering of mantle convection is possible, with catastrophic penetration events ("avalanches"), which affect the global flow field, once sufficient material has accumulated above the phase boundary (Machetel and Weber, 1991; Tackley et al., 1993; Solheim and Peltier, 1994). At lower Clapeyron slopes, the phase boundary has little effect in these global-scale models.

However, such global models generally do not fully capture the effects of plate strength and trench mobility. Many regional subduction models have documented that when trench retreat is possible or imposed, partial stagnation can already occur at relatively low Clapeyron slopes (from -0.5 to -1 MPa/K , i.e., well within the experimentally expected range) (Christensen, 1996; Torii and Yoshioka, 2007; Agrusta et al., 2017). This will be discussed further in Section 3.2.

The experiments from Agrusta et al. (2017) (Fig. 6) illustrate that in models where trenches are allowed to migrate freely, changing the Clapeyron slope of the postspinel transition between -0.5 and -3 MPa/K has a stronger effect on whether stagnation or partial stagnation occurs than changing the mantle viscosity jump between 5 and 30, although without a viscosity jump, stagnation is not easy to achieve either. These results agree with those from Yanagi-

sawa et al. (2010), who found in a 3-D spherical model with mobile trenches that a mix of stagnant and penetrating slabs is only created through the joint effect of a viscosity jump and endothermic phase boundary, where the latter is key in allowing stagnation and hence intermittent sinking of slabs into the lower mantle.

The exothermic phase transition expected at ~410 km depth when olivine transforms to its wadsleyite phase can encourage penetration, because it enhances slab sinking and piling in the transition zone (Christensen, 1996; Čížková et al., 2002; Běhouňková and Čížková, 2008). However, even with the effect of such an exothermic 410, slabs that can induce trench retreat can still get stalled by Γ as low as -1 MPa/K (Agrusta et al., 2017).

On the other hand, it has been proposed that the transition from olivine to wadsleyite may be kinetically delayed in the core of cold, i.e., old, slabs, to depths 200–300 km below the equilibrium depth. This would reduce the negative buoyancy of the oldest plates and aid their stagnation in the transition zone (Schmeling et al., 1999; Bina et al., 2001; Tetzlaff and Schmeling, 2009; Agrusta et al., 2014). The olivine component (in olivine, wadsleyite, or ringwoodite phase) makes up only ~60% of a peridotitic composition above 660 km. Experimental studies indicate that the pyroxene to garnet phase transitions in the remaining 40% of the composition, as well as in the crustal part of the slab, may be also be kinetically inhibited at typical slab temperatures (Hogrefe et al., 1994; Nishi et al., 2008; Van Mierlo et al., 2013). The delay of this transition, from its equilibrium depth between 200 and 300 km to possibly as deep as the base of the transition zone, adds so much buoyancy that it could aid the stagnation of both younger and older plates, although the effect should be stronger in the latter (Agrusta et al., 2014; King et al., 2015).

Near 660 km depth, it has been suggested that the effect of the ringwoodite to postspinel transition with a negative Clapeyron slope and the transition from garnet to bridgmanite, which also occurs near this depth and has a strongly positive Clapeyron slope, may largely cancel out any dynamic effects (Tackley et al., 2005). The depth range of the garnet transition and its Clapeyron slope are uncertain (Hirose, 2002; Xu et al., 2008; Stixrude and Lithgow-Bertelloni, 2011; Holland et al., 2013). In any case, the transition of the garnet components is rather diffuse and may spread over a depth interval as large as 100–250 km. The Clapeyron slope of the garnet transitions may also be low below ambient mantle temperatures. It is furthermore predicted to have a milder buoyancy effect than the transition of ringwoodite (Bina et al., 2001; Faccenda and Dal Zilio, 2017). It remains to be tested in regional subduction models with mobile trenches what the dynamic effect is of the interplay of these transitions. However, if the garnet transition spreads over a larger depth than the thickness of the slab, its effect would likely be significantly less than that of the olivine component transitions (Christensen and Yuen, 1985; Bina et al., 2001).

The modeling done so far, with a viscosity jump and a single endothermic phase transition at 660 km depth, strongly indicates that phase buoyancy plays a key role in causing slab stagnation. In our study (Agrusta et al., 2017) (where we used a $\Delta\rho_{\text{ph}}$ of 350 kg/m³, as appropriate for a 100% olivine composition), we found that at $\Delta\eta = \eta_{\text{LM}}/\eta_{\text{UM}} = 30$, old plates can stagnate for Γ stronger than

-0.7 to -0.8 MPa/K. For a pyrolitic density jump, this translates into a critical Clapeyron slope of -1.1 to -1.3 MPa/K. Thus partial stagnation is quite plausible for properties of the ringwoodite to postspinel transition well within the recently determined experimental range.

3.1.3. Density Jump

Although the most common assumption is that the whole mantle has a pyrolite-like composition (e.g., McDonough and Sun, 1995; Lyubetskaya and Korenaga, 2007)—with some amount of heterogeneity from recycled subducted slabs (Xu et al., 2008)—some studies have questioned this assumption. Discrepancies between the velocity and density jumps in spherical seismic models and estimates from experiments on phase transitions in olivine or pyrolite, as well as Earth evolution and geochemical and cosmochemical arguments have been used to advocate that there is an intrinsic chemical difference between upper and lower mantle (e.g., Stixrude et al., 1992; Khan et al., 2008; Javoy et al., 2010). If there is any chemical difference, it would need to result in a density jump at 660 km depth that is less than 6%, or else it would lead to fully layered mantle convection (Christensen and Yuen, 1984), which seismic tomography, plate evolution modeling, and considerations about the convective and thermal evolution of the Earth have shown is implausible (Silver et al., 1988; Ricard et al., 1993; Van der Hilst et al., 1997; McNamara and Van Keken, 2000). Furthermore, if it does not lead to layered convection, a chemical interface cannot survive over many convective cycles, although chemical gradients may persist (Van Keken and Zhong, 1999; Tackley et al., 2005; Brandenburg and Van Keken, 2007). For example, Ballmer et al. (2015) invoked compositional density gradients, due to a progressive enrichment in basaltic components with depth in the lower mantle, as a mechanism to stagnate slabs within the top of the lower mantle. Our compilation of transition-zone slab morphologies in Figure 2 shows, however, that slabs very rarely stagnate below 660, if at all.

3.2. Role of Slab Strength and Trench Motion

From the discussion above, it is already clear that trench retreat plays an important role in allowing some slabs to stagnate in the mantle transition zone, as was first proposed by Van der Hilst and Seno (1993). Trench motion turns out to be intimately linked to the strength of the subducting plate as it bends into the mantle. Furthermore, slab strength within the transition zone has been suggested to play a role in governing how easily slabs penetrate (Karato et al., 2001). Below we will discuss the role played by these slab-intrinsic factors and by trench mobility.

3.2.1. Role of Trench Motion

Most slabs actually do not just move in an along-dip direction but also exhibit retrograde motion (seaward away from the upper plate) that results in trench retreat (Elsasser, 1969; Chase, 1978; Garfunkel et al., 1986). Such retro-

grade motion is the consequence of vertical sinking of the plate, as expected for the most basic form of free subduction, driven by the slab's negative buoyancy and not significantly hampered by the upper plate or mantle convective forcing (Kincaid and Olson, 1987; Zhong and Gurnis, 1995; Becker et al., 1999; Funiciello et al., 2003a; Funiciello et al., 2003b; Schellart, 2008). Motivated by the free-subduction models of Kincaid and Olson (1987), Van der Hilst and Seno (1993) proposed that trench retreat could be responsible for the slab flattening as tomographically observed in the transition zone below the western Pacific.

Zhong and Gurnis's (1995) model that incorporates mobile plate boundaries clearly established that trench migration can produce slabs that stagnate over significant distances in the transition zone. Many other, regional-scale models prescribed trench motions and determined how much motion is required for flattening (Griffiths et al., 1995; Guillou-Frottier et al., 1995; Christensen, 1996; Olbertz et al., 1997; Čížková et al., 2002; Torii and Yoshioka, 2007). In this way, they inferred critical trench motions or dips. For example, Christensen (1996) found a critical retreat rate of 2–4 cm/yr. Further work indicates that the critical rate may scale with sinking velocity, i.e., a critical dip may be more appropriate, and furthermore, the cutoff depends on transition-zone resistance and likely also on slab strength (Torii and Yoshioka, 2007; Agrusta et al., 2017), so that there is not a single critical retreat rate.

Models in which trench motion develops dynamically show that variable trench mobility governed by slab internal and external forcing is the most likely cause for variable modes of subduction-transition zone interaction (e.g., Ribe, 2010; Stegman et al., 2010b; Čížková and Bina, 2013; Garel et al., 2014).

3.2.2. Subducting-Plate Density and Strength: Controls on Trench Motion

Models in which subduction and retreat velocities develop self-consistently have been used to study what factors control trench retreat, at first without any interface at the base of the upper mantle or with an impenetrable lower mantle, all without any forcing from an overriding plate. In such “free” subduction models, subduction usually involves trench retreat even if there is no boundary that hampers sinking at the base of the mantle (Ribe, 2010; Fourel et al., 2014).

The speed of trench retreat is controlled by subducting-plate strength and buoyancy (Bellahsen et al., 2005; Capitanio et al., 2007; Di Giuseppe et al., 2008; Schellart, 2008; Ribe, 2010; Stegman et al., 2010b; Capitanio and Morra, 2012; Fourel et al., 2014) (Fig. 7). Both high subducting-plate density and high resistance to bending at the trench encourage trench retreat. This can be understood as follows. The time that the plate has available to bend is controlled by its sinking rate, which again is governed by its density (slab pull). If the sinking time is too short to allow the plate to bend from a horizontal to a vertical geometry, the trench will retreat while the slab sinks. The stronger the resistance to bending, i.e., the higher the time that would be required to viscously bend the plate at the trench, the more retreat will occur.

In some models, slabs with high viscosity and low densities lead to trench advance (Bellahsen et al., 2005; Di Giuseppe et al., 2008; Funiciello et al., 2008; Stegman et al., 2010b). The advance occurs when plates are able to (i.e., have

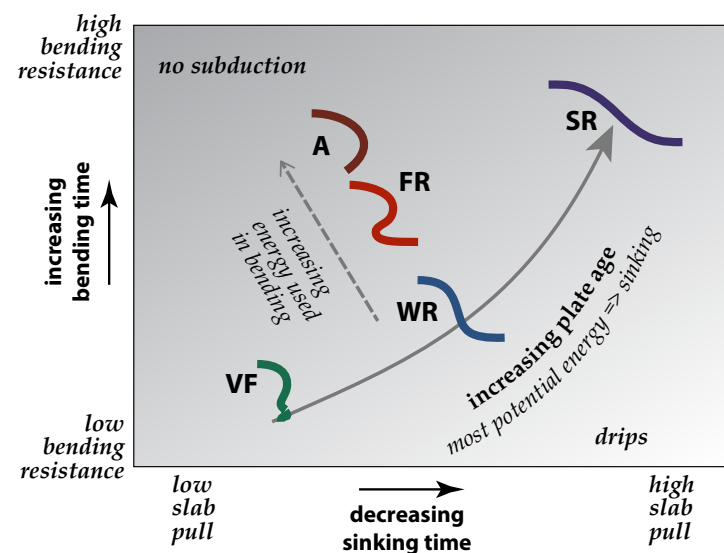


Figure 7. Schematic of how trench-motion modes are controlled by plate-bending resistance and slab pull, based on a range of free-subduction studies (Schellart, 2008; Ribe, 2010; Stegman et al., 2010b; Capitanio and Morra, 2012; Fourel et al., 2014). Modes are: VF—vertical folding with little trench motion; WR—weak trench retreat; SR—strong trench retreat; A—advancing trench; FR—fold and retreat. The style of subduction is the result of a competition between the time required to bend the plate at the trench and the time available to achieve this bending, which is controlled by the slab's upper-mantle sinking rate. Slabs with increasing age have higher density and larger strength and hence are increasingly able to drive trench retreat.

sufficient sinking time to) fully bend over but do not have a chance to unbend before reaching the base of the upper mantle (Ribe, 2010). Interaction of an overturned plate (dip $>90^\circ$) with a resisting upper- to lower-mantle interface triggers trench advance (Bellahsen et al., 2005; Funiciello et al., 2008; Schellart, 2008; Ribe, 2010). Weaker plates will unbend in response to the viscous mantle flow driven by the sinking and moving plate and thus arrive at the base of the upper mantle at an angle less than 90° . Strong and fast plates never bend beyond 90° . For a thermal aging trend of oceanic plates, density and viscosity will both increase, and retreating modes are expected to dominate. Furthermore, if the elastic effects on rheology are considered, plates unbend more easily, in particular when they have a higher viscosity (i.e., higher Maxwell time, which equals viscosity over the elastic Young's modulus) and hence behave more elastically (Farrington et al., 2014; Fourel et al., 2014). Therefore, the case of trench advance driven purely by the downgoing plate is probably not common on Earth. More likely, advance is the result of additional forcing either at the trailing end of the downgoing plate (like ridge push [Capitanio, 2013]) or from the upper plate or the arrival of buoyant features at the trench (Capitanio et al., 2010a; Magni et al., 2012; Fourel et al., 2014; Čížková and Bina, 2015; Goes et al., 2014).

Thermomechanical models (Garel et al., 2014; Agrusta et al., 2017) confirm that old plates, with high density and high viscosity have a higher propensity to retreat than younger plates. In principle, older plates should be less hampered by phase buoyancy, and indeed this is the behavior found in models of sinking plate segments of different thermal buoyancy (Ballmer et al., 2015). However, self-consistent subduction models show that their stronger tendency for retreat leads to older plates flattening and stagnating in the transition zone, while, for intermediate Clapeyron slopes and viscosity jumps less than 100, young plates tend to penetrate at relatively steep dips (Goes et al., 2008; Garel et al., 2014; Agrusta et al., 2017) (Fig. 6). Variations in plate age are thus a likely contributor to the observed variation in styles of slab transition zone interaction.

The insights into the role of subducting plate strength and buoyancy as the primary controls of trench motion have mostly come from 2-D models. In 3-D, additional variations in trench motion occur because of along-strike plate bending in response to flow around the plate edges (Funicello et al., 2006; Morra and Regenauer-Lieb, 2006; Schellart et al., 2007; Loiselet et al., 2009; Stegman et al., 2010a; Li and Ribe, 2012), leading to lower retreat of the plate edges and, for very wide plates, a trench stagnation point can develop in the center. Lateral changes in slab buoyancy can also lead to variations in trench motions, which depend on the scale of the features of different buoyancy and their relative contribution to overall slab pull (Martinod et al., 2005; Morra et al., 2006; Goes et al., 2008; Mason et al., 2010; Magni et al., 2014; Goes et al., 2014).

3.2.3. Role of Upper Plate and Mantle Resistance: External Controls on Trench Motion

Subduction zones are in reality never completely “free” to move, and it is a challenge to disentangle the respective roles and feedbacks of subducting versus neighboring plates (upper and side plates) dynamics. While the subducting plate generally drives trench motion, interplate coupling and upper-plate forcing provide resistance. In some cases, the upper plate may provide an additional driving force (Van Hunen et al., 2002; Arcay et al., 2008; Van Dinther et al., 2010; Čížková and Bina, 2015). Stronger plate coupling limits trench mobility and can, when high enough, even preclude subduction (De Franco et al., 2006; Běhouňková and Čížková, 2008; Androvičová et al., 2013) (Fig. 8). Upper-plate mobility depends not only on the forces that the plate experiences at its other boundaries, but in addition, thicker, more buoyant and longer overriding plates provide more resistance to trench motion (Zhong and Gurnis, 1997; Capitanio et al., 2010b; Van Dinther et al., 2010; Capitanio et al., 2011; Garel et al., 2014; Holt et al., 2015).

The effect of the upper plate is often studied by using kinematic conditions, most commonly by prescribing a fixed versus mobile trench (e.g., Čížková and Bina, 2013; Agrusta et al., 2017). The choice of kinematic conditions can lead to quite different slab stress patterns (Čížková et al., 2007), and it needs to be borne in mind that kinematic forcing may not allow the energetically

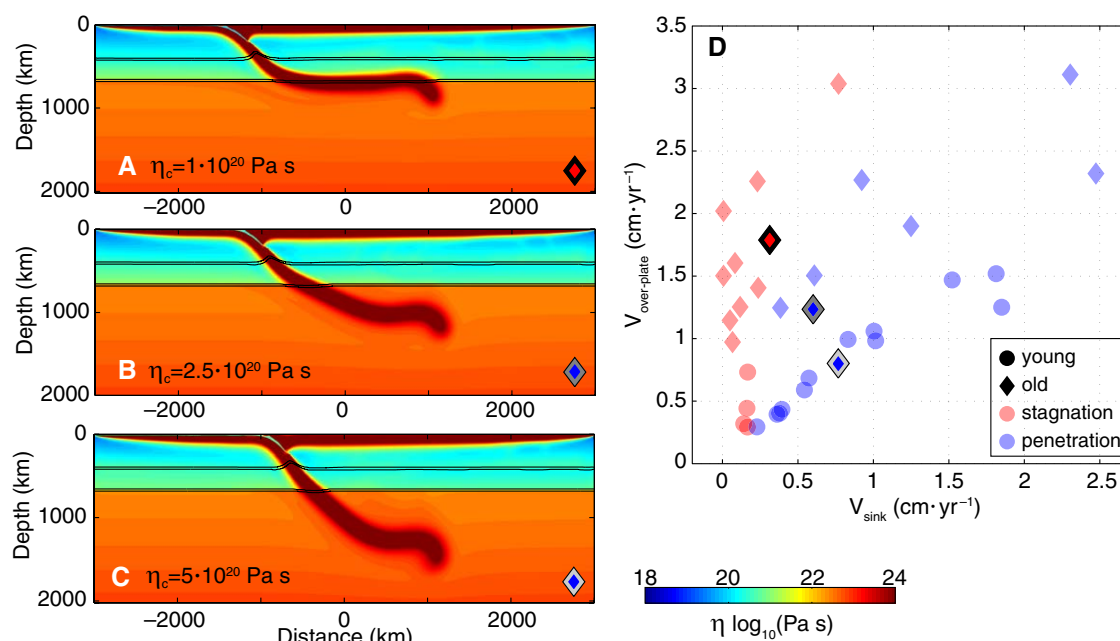


Figure 8. Illustration of how trench mobility can affect whether slabs penetrate or stagnate. (Left) In these cases, the mobility of the trench is modulated by changing the viscosity, η_c , of the crustal layer on top of the subducting plate, which governs the coupling between the two plates. The models shown are variations of a model where an old plate interacts with a viscosity jump of 20 and a postspinel transition with Clapeyron slope of -2 MPa/K (red triangle in Fig. 6). (A) For a reference trench mobility $\eta_c = 1 \cdot 10^{20}$ Pa s; (B) for a less mobile trench with $\eta_c = 2.5 \cdot 10^{20}$ Pa s; (C) for the least mobile trench with $\eta_c = 5 \cdot 10^{20}$ Pa s. Colors represent viscosity, and black lines represent the depths at which 1% and 99% of the olivine to wadsleyite (near 400 km depth) and postspinel (near 660 km depth) transitions are complete. (Right, D) The trench ($V_{\text{over-plate}}$) and lower-mantle slab sinking (V_{sink}) velocities of the cases in A, B, and C are compared to those of the cases investigated by Agrusta et al. (2017) and summarized in Figure 6, where a single crustal viscosity, $1 \cdot 10^{20}$ Pa s, was used and Clapeyron slopes and viscosity jumps were varied. Stagnant slabs have relatively high trench retreat velocities for their lower-mantle sinking velocities. By increasing crustal viscosity, trench retreat is reduced and lower-mantle sinking enhanced, and the interaction mode can change from stagnation (A) to just penetrating while still flattening (B) to easily penetrating (C).

most favorable modes of subduction (Han and Gurnis, 1999). In models where the trench is held fixed, higher slab strength is found to encourage penetration (Zhong and Gurnis, 1994; Arredondo and Billen, 2016), contrasting with dynamic trench-motion models where higher slab strength aids trench retreat and slab flattening (e.g., Zhong and Gurnis, 1995; Capitanio et al., 2007).

Trench retreat is not a consequence of the slab's interaction with an interface that hampers sinking. However, trench motion is enhanced and modulated by interaction with a viscosity and/or phase change (Becker et al., 1999; Bellahsen et al., 2005; Capitanio et al., 2010b; Čížková and Bina, 2013; Garel et al., 2014; Agrusta et al., 2017). As the slab accumulates in the transition zone, alternating phases of somewhat higher and lower retreat velocities (with accompanying changes in dip) tend to develop (Capitanio et al., 2010b; Lee and King, 2011; Čížková and Bina, 2013; Garel et al., 2014). These fluctuations are an expression of slab buckling, because even where the slab flattens at the base of the transition zone, the deformation is essentially a buckling response (Houseman and Gubbins, 1997; Ribe et al., 2007), as is seen most clearly in models with weaker slabs or ones where sinking is enhanced (Lee and King, 2011; Čížková and Bina, 2013; Cerpa et al., 2014). Trench-motion fluctuations due to buckling can be enhanced if the upper plate can break and heal (Clark et al., 2008). Models where the slab buckles in its interaction with the transition zone produce variations in upper-plate stress on time scales similar to those observed in, for example, the Andes or backarc spreading phases for Tonga (Clark et al., 2008; Capitanio et al., 2010b; Lee and King, 2011).

3.2.4. Slab Strength in the Transition Zone

Karato et al. (2001) proposed that slab weakening in the transition zone associated with small grain size around a wedge of metastable olivine in the slab's core may be key for trapping slab material in the transition zone and that this would be most effective for intermediate age slabs, which are hot and thin enough to bend but with a core that is cold enough to induce a sluggish olivine-to-wadleyite phase transition. Čížková et al. (2002) tested the effect of weakening the slab in the transition zone and found it was secondary to that of trench motion. King and Ita (1995) also found that slab strength does not exert a major influence on whether slabs penetrate or not, when the trench is free to move. Others further tested the effect of local slab weakening in the transition zone and confirmed that the effect is not dominant, but it may be sufficient to stagnate a slab that is otherwise marginally penetrating (Tagawa et al., 2007; Agrusta et al., 2017). The buckling of weaker slabs can actually increase the slab's Stokes' sinking velocity (which scales with diameter squared) and hence help it penetrate a high-viscosity lower mantle rather than stagnating it. These results imply that strength of the subducting plate at the trench is much more important in controlling how slabs interact with the transition zone than any changes in slab strength within the transition zone.

Several studies did find that over the longer term, weakening helps stagnant slabs destabilize and flush into the lower mantle (Nakakuki et al., 2010; Agrusta et al., 2017). This flushing is akin to a Rayleigh-Taylor instability, for

which it is well established that it is facilitated by lower viscosities. Several studies have found that such stagnant slab destabilization can affect mantle flow and overlying plate velocities (Pysklywec et al., 2003; Pysklywec and Ishii, 2005; Motoki and Ballmer, 2015) (see further in Section 4.2).

3.2.5. Changing Trench Mobility

Aging of the subducting plate and the consequence of this on trench mobility can result in a change in transition-zone dynamics in time, from penetration to stagnation (Agrusta et al., 2017). This would lead to a flat-slab morphology with a leading end that has entered the deep mantle. The opposite switch is not as easily induced, but decreasing plate age at the trench does lead to decreased trench motion and can under certain conditions trigger lower-mantle sinking of a previously stagnated slab. Detachment of such increasingly buoyant slabs can facilitate the start of lower-mantle sinking (Agrusta et al., 2017). This switch would lead to slabs that start entering the lower mantle at the hinge between dipping and flattened slab segments as shown in Figure 9C. Changing the upper-plate resistance to trench motion can be a quite efficient mechanism to induce switches from penetration to stagnation as well as vice versa (Agrusta et al., 2017). However, regional models usually test kinematic extremes of upper-plate forcing (either fixed, free, or forced upper plates), and the effects may be more subtle or different in a global dynamic system.

4. COMBINING MODELS AND OBSERVATIONS

4.1. Variable Styles of Slab Transition Zone Interaction

Dynamic modeling identifies variable trench motions as the most probable cause for the different ways in which slabs interact with the transition zone (Section 3). This proposed link is consistent with the observation that slab morphology correlates well with the history of trench motions (Fig. 4). Furthermore, the models predict the largest trench motions for the oldest densest plates, and indeed, although trench motions do not simply follow an age trend (Sdrolias and Müller, 2006; Goes et al., 2011) (Fig. 3), the largest trench velocities have been found to occur for plates older than ~50 m.y. (Molnar and Atwater, 1978; Sdrolias and Müller, 2006; Goes et al., 2011), and slabs of old plates seem to stagnate more often than young plate slabs (King et al., 2015; Section 2.1). This indicates that the forcing by downgoing plates older than ~50 m.y. is generally sufficiently large to overcome other forces (e.g., by the upper plate or the convective mantle) that may impede trench motions, consistent with the long-standing conclusion that the downgoing plate pull is the primary force driving plate motions (Forsyth and Uyeda, 1975; Zahirovic et al., 2015). A recent global dynamic modeling study also concluded that subducting plates provide the main forces that drive formation and migration of plate boundaries (Mallard et al., 2016).

Variations in slab transition zone interaction in space and time are thus likely the consequence of variations in trench mobility, which can be caused by

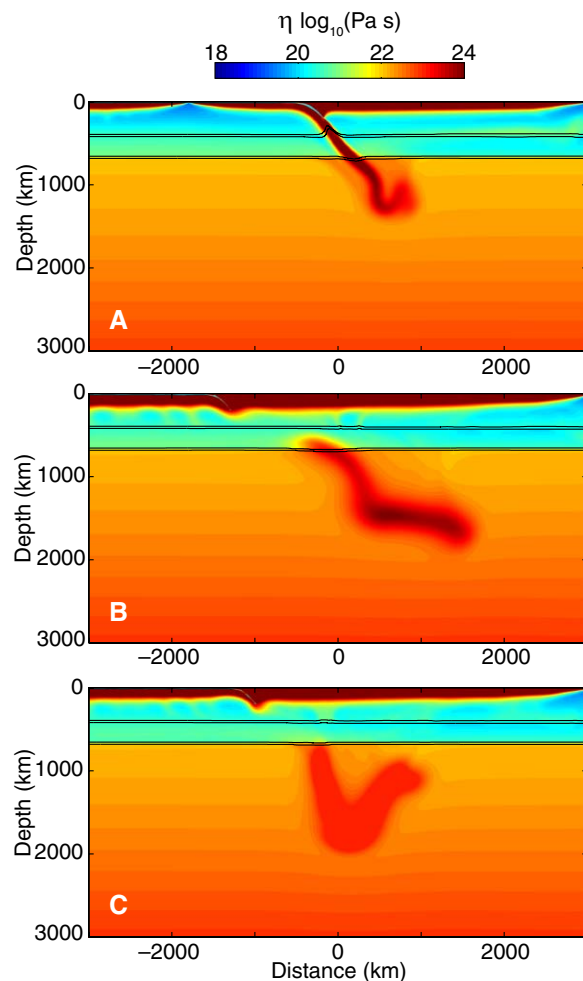


Figure 9. Some examples of the lower-mantle slab shapes that develop in the thermo-mechanical subduction models of Agrusta et al. (2017). (A) Penetrating slab that buckles and thickens as it enters the lower mantle. (B) Previously flattened slab that starts sinking into the lower mantle and maintains a relatively flat geometry during its sinking through the upper half of the lower mantle. (C) Previously flattened slab that starts sinking into the lower mantle at the hinge and folds double on its way down through the lower mantle. At the start of the models, the trench was located at $x = 0$, i.e., the slab tip can end up sinking at a distance 1000–1500 km offset from where the slab started sinking.

either changes in the downgoing-plate driving force (e.g., due to variations in plate age or arrival of buoyant features on the subducting plate at the trench) or by changes in the forces that constrain or force trench motion, e.g., by the upper plate (Agrusta et al., 2017). For example, the arrival of continental material at the trench has been shown to be able to induce trench advance (Magni et al., 2012), like that observed for the trench north of India. Thus the start of continental collision may be responsible for a switch from a retreating subduction mode, which has been proposed to explain lower-mantle slab anomalies below India (Hafkenscheid et al., 2006), to the Cenozoic advancing mode (Capitanio et al., 2010a). Similarly, arrival of the Australian continent at the Banda

trench may have halted its trench retreat and induced the sinking of a slab segment that previously flattened in the transition zone. On the other hand, the aging of the Pacific plate as it subducted along the Tonga and Japan trenches during the Cenozoic may have led to the change from penetrating to stagnating subduction that has been inferred from seismic tomography (Van der Hilst, 1995; Goes et al., 2008) (Fig. 2).

4.2. Time Scales of Slab Stagnation

Several previous studies have noted that transition-zone slabs will only remain stagnant for a limited amount of time (Zhong and Gurnis, 1995; Christensen, 1996; Pysklywec and Ishii, 2005; Nakakuki et al., 2010; King et al., 2015). As slabs warm up, phase boundary topography reduces and hence phase buoyancy decreases, while the slab's density anomaly diffuses, although the overall integrated thermal density anomaly decreases only very slowly (Turcotte and Schubert, 1982). The diffusion time scale over which the slabs warm sufficiently to make the phase buoyancy effect too small to keep a slab stagnant has been estimated to ~250–300 m.y. (Christensen, 1996). As a slab warms up, it will also weaken, which further facilitates its deformation and destabilization (Nakakuki et al., 2010).

As soon as part of the slab sinks below the phase boundary, that part will be gravitationally unstable and can eventually pull the rest of the slab along into the lower mantle. Various regional-scale models, with or without free trench motion, show that if slabs have a similar strength to that of the surrounding (lower) mantle, they can destabilize in a few tens of millions of years (Griffiths et al., 1995; Zhong and Gurnis, 1995; Nakakuki et al., 2010; Motoki and Ballmer, 2015), while slabs that have viscosities that exceed those of their surroundings by about two orders of magnitude take between 100 and over 300 million years to destabilize (Zhong and Gurnis, 1995; Nakakuki et al., 2010; Agrusta et al., 2017). It would be expected that, due to the Arrhenius temperature sensitivities of mantle flow laws (Ranalli, 1995), the colder slab has a higher viscosity than its surroundings. The occurrence of some earthquakes in the flat parts of slabs (Lundgren and Giardini, 1994) is an indication that they are indeed stronger than the surrounding mantle, because the seismicity requires that at least some flat-slab segments retain sufficient strength to allow elastic energy accumulation. Furthermore, although grain-size reduction at a metastable phase transition may lead to weakening of the slab core (Karato et al., 2001), this is unlikely to persist into the stagnant slab. This implies that the time scales of destabilization are probably closer to several hundred million years.

Such time scales are much longer than the time scales of stagnation estimated from the seismically imaged volume of material in the transition zone, which range from ~20–60 m.y., even if some amount of buckling is accounted for (Section 2.1) (Tajima and Grand, 1998; Schmid et al., 2002). This would indicate that penetration is commonly triggered before the stagnant slab becomes negatively buoyant (Agrusta et al., 2017).

It has been suggested from models (Zhong and Gurnis, 1995; Tackley et al., 2005) and observations (Goes et al., 2008) that the sinking of previously stag-

nant slabs leads to large increases in subducting-plate velocities. However, as discussed in Section 3.2, neither global nor regional models (e.g., Christensen, 1996; Yanagisawa et al., 2010) confirm that for the postspinel Clapeyron slopes most likely in the mantle, lower-mantle sinking of previously stagnant slabs is associated with large peaks in plate velocities. Some regional plate acceleration by up to a factor of 2 can occur (Christensen, 1996; Pysklywec and Ishii, 2005; Nakakuki et al., 2010; Agrusta et al., 2017), and this may explain some of the plate motions that are relatively high for their slab's buoyancy (as identified by Goes et al. [2008]), such as that of the subduction below Japan in the early Cenozoic. However, the high Mesozoic velocities for the motion of India and early Cenozoic motions for the Farallon plate exceed current average velocities by a factor of 2–4 and, hence, probably require an additional driving mechanism, e.g., an increase convective vigor due to the lowering of viscosity by the influx of hot material from depth and/or the development of a large whole-mantle-scale convective cell (Becker and Faccenna, 2011; Cande and Stegman, 2011; van Hinsbergen et al., 2011).

4.3. Lower-Mantle Slab Morphology

As discussed in Section 1.3, once slabs enter the lower mantle, they appear to thicken, by as much as a factor 2–5. Models predict significant buckling and thereby thickening when the viscosity contrast encountered by the slabs at the base of the transition zone is at least a factor of 20 or 30 (Gurnis and Hager, 1988; Gaherty and Hager, 1994; King, 2002; Běhounková and Čížková, 2008; Lee and King, 2011; Čížková and Bina, 2013). The increase in slab pull due to a shallowing olivine to wadsleyite phase transition in the slab ~400 km depth may enhance buckling (Běhounková and Čížková, 2008). Finally, some amount of transition-zone slab buckling is consistent with focal mechanisms (e.g., Myhill, 2012), as well as with high seismic strain rates inferred for the Tonga slab (Giardini and Woodhouse, 1984; Bevis, 1988; Holt, 1995).

The ability to buckle and thicken puts a limit on transition-zone slab strength, which should not be stronger than ~2–3 orders of magnitude higher viscosity, or a yield stress of 100–300 MPa (Houseman and Gubbins, 1997; Běhounková and Čížková, 2008; Lee and King, 2011). Effective slab viscosities of ~2 orders of magnitude higher than the surrounding mantle are also most consistent with the geoid signal of subduction zones (King and Hager, 1994; Moresi and Gurnis, 1996; Zhong and Davies, 1999). On the other hand, the existence of deep Benioff zones requires that those slabs retain sufficient strength to store elastic energy. This may require that slabs have an effective viscosity at least 2–3 orders of magnitude higher than that of the surrounding mantle (Fourel et al., 2014), i.e., a strength near the upper bound defined by the other constraints.

Upon sinking, all slabs will develop a more rounded form because they try to achieve a shape that sinks more efficiently than the planar geometry they start subducting with (Jarvis and Lowman, 2007; Loiselet et al., 2010). For simple vertical sinkers, this is achieved by rounding and widening of the leading edge (Jarvis and Lowman, 2007; Loiselet et al., 2010). For flattened slabs, this

may be achieved by folding. Some examples of how slabs evolve their shapes while sinking in the transition zone are shown in Figure 9. A combination of buckling, folding, rounding, and diffusive widening leads to a significant change in slab shape as they sink through the lower mantle. Note that stagnant slab shapes may be preserved for a while as such slabs start sinking into the lower mantle (Fig. 9B). This could be an explanation for the apparent flat slab at 1100 km depth below Borneo. Folding slabs have not been proposed previously; however, it may be worth re-examining some complex or broad high-velocity anomalies below the transition zone in this light (e.g., those from Sigloch [2011] below North America).

In comparing plate reconstructions with tomography, it is often assumed that the mantle anomalies reside more or less (within ~500 km) below the location of the trench where the slab originally subducted (Van der Meer et al., 2009; Sigloch and Mihalynuk, 2013). However, models show that upon sinking into the lower mantle, previously stagnant slabs may end up as far as 1000–2000 km displaced laterally from where they originally subducted (Billen, 2008; Garel et al., 2014; models in Fig. 9). Both the shape evolution and lateral displacement that accompany it will make it more challenging to relate lower-mantle anomalies to plate-motion histories and increasingly so with depth, which may explain the difficulty of correlating plate-motion histories with the deepest mantle structures (Domeier et al., 2016).

5. SUMMARY

Seismic tomography and Benioff seismicity highlight that subducting slabs encounter resistance to sinking in the transition zone and that they can respond to this resistance by either buckling and thickening before they sink into the lower mantle or by flattening and apparently stagnating at the base of the transition zone over distances of 500–2000 km for 20–60 m.y. From modeling and observational studies over the past 50 years, we now have a quite good understanding about what governs this behavior and what its implications are for plate motions and time scales of mantle mixing. A summary of the main insights:

1. When slabs stagnate, they mainly do so above 700 km depth (Fig. 2). Very few, if any, are flat in the upper part of the lower mantle. Slabs that appear flattened in the shallow lower mantle are sometimes only apparently flat (when the cross sections studied are oblique to the actual structures) or may represent slabs that previously flattened in the transition zone and subsequently started sinking through.
2. An increase in viscosity at the base of the transition zone by a factor 20–50 provides sufficient resistance to sinking to induce slab buckling and/or trench retreat. Such an increase in viscosity also explains the dominance of downwind compression below 300 km depth seen in Benioff seismicity globally (Vassiliou and Hager, 1988; Alpert et al., 2010), as well as the local geoid signature around subduction zones (Chen and King, 1998; King, 2002;

- Tosi et al., 2009). It does not, however, sufficiently stagnate slabs to accumulate flat slabs of up to 2000 km long (Garel et al., 2014).
3. The endothermic ringwoodite to postspinel phase change takes place at a larger depth in the cold slab than in the surrounding mantle, thus providing the additional buoyancy that can make slabs flatten over distances >1000 km and stagnate in the upper mantle over time scales of several tens of millions of years or more (Yanagisawa et al., 2010; Agrusta et al., 2017). However, for the likely values of the Clapeyron slope of this transition (between -0.5 and -2 MPa/K), stagnation only occurs when trench retreat is possible (Yanagisawa et al., 2010; Agrusta et al., 2017).
 4. The variable style of slab transition zone interaction on Earth is governed by variations in trench mobility. Dynamic subduction models show that subduction accompanied by trench retreat is the most basic form of subduction (Kincaid and Olson, 1987). Trench motion is controlled by downgoing plate buoyancy and strength (Bellahsen et al., 2005; Capitanio et al., 2007; Tagawa et al., 2007; Ribe, 2010) and by upper-plate deformability and mobility (Garel et al., 2014; Holt et al., 2015). As a result, old strong slabs have a stronger tendency to retreat than young weak slabs (Agrusta et al., 2017). Indeed, most trenches on Earth retreat, and when integrated over the Cenozoic, all of the major trenches retreated, with the exception of the Himalayan front, which advanced in response to the continental collision. That downgoing plate buoyancy plays a key role is further borne out by the observation that significant trench motions are only observed for relatively old (>50 m.y.) subducting plates (Molnar and Atwater, 1978; Sdrolias and Müller, 2006).
 5. The upper-mantle slabs imaged by Benioff seismicity and seismic tomography correspond to subduction of the past 15–60 m.y. (Fig. 2). Because thermal assimilation of slabs takes on the order of several hundred million years, this is a strong indication that earlier subducted slabs have sunk into the lower mantle. Indeed lower-mantle, high seismic-velocity anomalies can mostly be correlated with Mesozoic to early Cenozoic plate-motion histories (Ricard et al., 1993; Grand, 1994; Van der Meer et al., 2009).
 6. Modeling shows that slabs once stagnated above a viscosity and phase transition take 100–300 m.y. to destabilize (Christensen, 1996). This implies that in natural subduction, lower-mantle penetration is generally triggered. Such triggering can be induced by changes in slab buoyancy (e.g., due to changing age or the arrival of continental lithosphere at the trench) or in resistance to upper-plate motion (Agrusta et al., 2017). Irrespective of whether lower-mantle sinking is triggered or evolves independently, models do not predict that the deeper sinking of previously flattened slabs is accompanied by large fluctuations in plate velocities (Christensen, 1996; Pysklywec and Ishii, 2005; Yanagisawa et al., 2010; Agrusta et al., 2017). Hence periods of much higher subduction velocities (e.g., India and Farallon before 50 m.y.) are likely the result of a different mechanism, e.g., deep subduction in conjunction with forcing by plumes (Becker and Faccenna, 2011; Cande and Stegman, 2011; van Hinsbergen et al., 2011).
 7. Once slabs sink into the lower mantle, they will slowly lose their linear shape, either by folding and/or bulk thickening and rounding. This and the

fact that slabs may end up as far as 1000–2000 km from the position where they originally subducted, makes associating lower-mantle slabs with past trenches more difficult with increasing depth in the mantle. This has indeed been noted in studies that have tried to correlate plate-motion history with tomographic anomalies in the lower mantle (Domeier et al., 2016).

8. These insights in slab transition zone interaction indicate that, at present, mixing between upper and lower mantle is at most delayed by a few tens of millions of years. On the time scale of 100–200 m.y., most subducted material is expected to sink into the lower mantle. It has been suggested that mixing across an endothermic phase boundary may have been less efficient in an earlier hotter Earth, due to the higher Rayleigh number (Christensen and Yuen, 1985; Davies, 1995). However, hotter plates would likely have been younger and thinner and thus less able to drive trench retreat, and hence the role of the transition zone in hotter Earth mixing may need re-evaluation (Agrusta et al., 2016).

ACKNOWLEDGMENTS

Thanks to all those we have had discussions with over the years, which helped shape our ideas in this paper, in particular, Hana Čížková, Fabio Capitanio, Claudio Faccenna, Francesca Funicello, Loïc Fourel, Rhodri Davies, and Huw Davies. We also thank Scott King and an anonymous reviewer for their thoughtful comments on the manuscript. This work was funded by Natural Environment Research Council (NERC; grants NE/J008028/1 and NE/I024429/1) and made use of the facilities of N8 High Performance Computing provided and was funded under the embedded CSE program of the ARCHER UK National Supercomputing Service (<http://www.archer.ac.uk>). RA and JvH also acknowledge funding from the European Research Council (grant ERC StG 279828).

REFERENCES CITED

- Agrusta, R., van Hunen, J., and Goes, S., 2014, The effect of metastable pyroxene on the slab dynamics: *Geophysical Research Letters*, v. 41, p. 8800–8808, doi:10.1002/2014GL062159.
- Agrusta, R., Goes, S., and van Hunen, J., 2016, Subducting-slab transition zone interaction: Stagnation, penetration and mode switches: *Eos (Transactions, American Geophysical Union)*, D131B-2638.
- Agrusta, R., Goes, S., and van Hunen, J., 2017, Subducting-slab transition zone interaction: stagnation, penetration and mode switches: *Earth and Planetary Science Letters*, v. 464, p. 10–23, doi:10.1016/j.epsl.2017.02.005.
- Alisic, L., Gurnis, M., Stadler, G., Burstedde, C., Wilcox, L., and Ghattas, O., 2010, Slab stress and strain rate as constraints on global mantle flow: *Geophysical Research Letters*, v. 37, L22308, doi:10.1029/2010GL045312.
- Alpert, L.A., Becker, T.W., and Bailey, I.W., 2010, Global slab deformation and centroid moment tensor constraints on viscosity: *Geochemistry, Geophysics, Geosystems*, v. 11, Q12006, doi:10.1029/2010GC003301.
- Androvičová, A., Čížková, H., and Van den Berg, A., 2013, The effects of rheological decoupling on slab deformation in the Earth's upper mantle: *Studia Geophysica et Geodaetica*, v. 57, p. 460–481, doi:10.1007/s11200-012-0259-7.
- Apperson, K.D., and Frohlich, C., 1987, The relationship between Wadati-Benioff Zone geometry and P, T and B axes of intermediate and deep focus earthquakes: *Journal of Geophysical Research*, v. 92, p. 13,821–13,831, doi:10.1029/JB092iB13p13821.
- Arcay, D., Lallemand, S., and Doin, M.-P., 2008, Back-arc strain in subduction zones: Statistical observations versus numerical modeling: *Geochemistry, Geophysics, Geosystems*, v. 9, no. 5, Q05015, doi:10.1029/2007GC001875.
- Arredondo, K.M., and Billen, M.I., 2016, The effects of phase transitions and compositional layering in two-dimensional kinematic models of subduction: *Journal of Geodynamics*, v. 100, p. 159–174, doi:10.1016/j.jog.2016.05.009.

- Bailey, I.W., Alpert, L.A., Becker, T., and Miller, M.S., 2012, Co-seismic deformation of deep slabs based on summed CMT data: *Journal of Geophysical Research*, v. 117, B04404, doi:10.1029/2011JB008943.
- Ballmer, M.D., Schmerr, N.C., Nakagawa, T., and Ritsema, J., 2015, Compositional mantle layering revealed by slab stagnation at ~1000-km depth: *Science Advances*, v. 1, no. 11, e1500815, doi:10.1126/sciadv.1500815.
- Barker, P.F., 2001, Scotia Sea regional tectonic evolution: Implications for mantle flow and palaeo-circulation: *Earth-Science Reviews*, v. 55, p. 1–39, doi:10.1016/S0012-8252(01)00055-1.
- Becker, T.W., and Faccenna, C., 2011, Mantle conveyor beneath the Tethyan collisional belt: *Earth and Planetary Science Letters*, v. 310, p. 453–461, doi:10.1016/j.epsl.2011.08.021.
- Becker, T.W., Faccenna, C., and O'Connell, R.J., 1999, The development of slabs in the upper mantle: Insights from numerical and laboratory experiments: *Journal of Geophysical Research*, v. 104, no. B7, p. 15,207–15,226, doi:10.1029/1999JB900140.
- Běhounková, M., and Čížková, H., 2008, Long-wavelength character of subducted slabs in the lower mantle: *Earth and Planetary Science Letters*, v. 275, p. 43–53, doi:10.1016/j.epsl.2008.07.059.
- Bellahsen, N., Faccenna, C., and Funiello, F., 2005, Dynamics of subduction and plate motion in laboratory experiments: Insights into the “plate tectonics” behavior of the Earth: *Journal of Geophysical Research*, v. 110, B01401, doi:10.1029/2004JB002999.
- Bevis, M., 1988, Seismic slip and down-dip strain rates in Wadati-Benioff zones: *Science*, v. 240, p. 1317–1319, doi:10.1126/science.240.4857.1317.
- Bijwaard, H., Spakman, W., and Engdahl, E.R., 1998, Closing the gap between regional and global travel time tomography: *Journal of Geophysical Research*, v. 103, p. 30,055–30,078, doi:10.1029/98JB02467.
- Billen, M.I., 2008, Modeling the dynamics of subducting slabs: *Annual Review of Earth and Planetary Sciences*, v. 36, p. 325–356, doi:10.1146/annurev.earth.36.031207.124129.
- Bina, C.R., Stein, S., Marton, F.C., and Van Ark, E.M., 2001, Implications of slab mineralogy for subduction dynamics: *Physics of the Earth and Planetary Interiors*, v. 127, p. 51–66, doi:10.1016/S0031-9201(01)00221-7.
- Brandenburg, J.P., and Van Keken, P.E., 2007, Deep storage of oceanic crust in a vigorously convecting mantle: *Journal of Geophysical Research*, v. 112, B06403, doi:10.1029/2006JB004813.
- Bunge, H.P., and Grand, S.P., 2000, Mesozoic plate motion history below the northeast Pacific Ocean from seismic images of the subducted Farallon slab: *Nature*, v. 405, p. 337–340, doi:10.1038/35012586.
- Butterworth, N.P., Talsma, A.S., Müller, R.D., Seton, M., Bunge, H.-P., Schubert, B., Shephard, G.E., and Heine, C., 2014, Geological, tomographic, kinematic and geodynamic constraints on the dynamics of sinking slabs: *Journal of Geodynamics*, v. 73, p. 1–13, doi:10.1016/j.jog.2013.10.006.
- Cande, S.C., and Stegman, D.R., 2011, Indian and African plate motions driven by the push force of the Réunion plume head: *Nature*, v. 475, p. 47–52, doi:10.1038/nature10174.
- Capitanio, F.A., 2013, Lithospheric-age control on the migrations of oceanic convergent margins: *Tectonophysics*, v. 593, p. 193–200, doi:10.1016/j.tecto.2013.03.003.
- Capitanio, F.A., and Morra, G., 2012, The bending mechanics in a dynamic subduction system: Constraints from numerical modelling and global compilation analysis: *Tectonophysics*, v. 522–523, p. 224–234, doi:10.1016/j.tecto.2011.12.003.
- Capitanio, F.A., Morra, G., and Goes, S., 2007, Dynamic models of downgoing plate buoyancy driven subduction: Subduction motions and energy dissipation: *Earth and Planetary Science Letters*, v. 262, p. 284–297, doi:10.1016/j.epsl.2007.07.039.
- Capitanio, F.A., Morra, G., Goes, S., Weinberg, R.F., and Moresi, L., 2010a, India-Asia convergence driven by the subduction of the Greater Indian continent: *Nature Geoscience*, v. 3, p. 136–139, doi:10.1038/ngeo725.
- Capitanio, F.A., Stegman, D.R., Moresi, L.N., and Sharples, W., 2010b, Upper-plate controls on deep subduction, trench migration and deformation at convergent margins: *Tectonophysics*, v. 483, p. 80–92, doi:10.1016/j.tecto.2009.08.020.
- Capitanio, F.A., Faccenna, C., Zlotnik, S., and Stegman, D.R., 2011, Subduction dynamics and the origin of Andean orogeny and the Bolivian orocline: *Nature*, v. 480, p. 83–86, doi:10.1038/nature10596.
- Carlson, R.L., Hilde, T.W.C., and Uyeda, S., 1983, The driving mechanism of plate tectonics: relation to age of the lithosphere at trenches: *Geophysical Research Letters*, v. 10, no. 4, p. 297–300, doi:10.1029/GL010i004p00297.
- Carminati, E., and Petricca, P., 2010, State of stress in slabs as a function of large-scale plate kinematics: *Geochemistry, Geophysics, Geosystems*, v. 11, Q04006, doi:10.1029/2009GC003003.
- Cerpa, N.G., Hassani, R., Gerbault, M., and Prévost, J.-H., 2014, A fictitious domain method for lithosphere-asthenosphere interaction: Application to periodic slab folding in the upper mantle: *Geochemistry, Geophysics, Geosystems*, v. 15, p. 1852–1877, doi:10.1002/2014GC005241.
- Chase, C.G., 1978, Extension behind island arcs and motions relative to hot spots: *Journal of Geophysical Research*, v. 83, p. 5385–5387, doi:10.1029/JB083iB11p05385.
- Chen, J., and King, S.D., 1998, The influence of temperature and depth dependent viscosity on geoid and topography profiles from models of mantle convection: *Physics of the Earth and Planetary Interiors*, v. 106, p. 75–92, doi:10.1016/S0031-9201(97)00110-6.
- Christensen, U.R., 1996, The influence of trench migration on slab penetration into the lower mantle: *Earth and Planetary Science Letters*, v. 140, no. 1–4, p. 27–39, doi:10.1016/0012-821X(96)00023-4.
- Christensen, U.R., 2001, Geodynamic models of deep subduction: *Physics of the Earth and Planetary Interiors*, v. 127, p. 25–34, doi:10.1016/S0031-9201(01)00219-9.
- Christensen, U.R., and Yuen, D.A., 1984, The interaction of a subducting lithosphere slab with a chemical or phase boundary: *Journal of Geophysical Research*, v. 89, B6, p. 4389–4402, doi:10.1029/JB089iB06p04389.
- Christensen, U.R., and Yuen, D.A., 1985, Layered convection induced by phase transitions: *Journal of Geophysical Research*, v. 90, p. 10,291–10,300, doi:10.1029/JB090iB12p10291.
- Čížková, H., and Bina, C.R., 2013, Effects of mantle and subduction-interface rheologies on slab stagnation and trench rollback: *Earth and Planetary Science Letters*, v. 379, p. 95–103, doi:10.1016/j.epsl.2013.08.011.
- Čížková, H., and Bina, C.R., 2015, Geodynamics of trench advance: Insights from a Philippine-Sea-style geometry: *Earth and Planetary Science Letters*, v. 430, p. 408–415, doi:10.1016/j.epsl.2015.07.004.
- Čížková, H., van Hunen, J., van der Berg, A.P., and Vlaar, N.J., 2002, The influence of rheological weakening and yield stress on the interaction of slabs with the 670 km discontinuity: *Earth and Planetary Science Letters*, v. 199, no. 3–4, p. 447–457, doi:10.1016/S0012-821X(02)00586-1.
- Čížková, H., van Hunen, J., and Van den Berg, A., 2007, Stress distribution within subducting slabs and their deformation in the transition zone: *Physics of the Earth and Planetary Interiors*, v. 161, no. 3–4, p. 202–214, doi:10.1016/j.pepi.2007.02.002.
- Čížková, H., Van den Berg, A., Spakman, W., and Matyska, C., 2012, The viscosity of Earth's lower mantle inferred from sinking speed of subducted lithosphere: *Physics of the Earth and Planetary Interiors*, v. 200–201, p. 56–62, doi:10.1016/j.pepi.2012.02.010.
- Clark, S.R., Stegman, D.R., and Müller, R.D., 2008, Episodicity in back-arc tectonic regimes: *Physics of the Earth and Planetary Interiors*, v. 171, p. 265–279, doi:10.1016/j.pepi.2008.04.012.
- Cloos, M., 1993, Lithospheric buoyancy and collisional orogenesis: Subduction of oceanic plateaus, continental margins, island arcs, spreading ridges, and seamounts: *Geological Society of America Bulletin*, v. 105, p. 715–737, doi:10.1130/0016-7606(1993)105<0715:LBACOS>2.3.CO;2.
- Conrad, C.P., and Lithgow-Bertelloni, C., 2002, How mantle slabs drive plate tectonics: *Science*, v. 298, no. 5591, p. 207–209, doi:10.1126/science.1074161.
- Davaille, A., and Jaupart, C., 1994, Onset of thermal convection in fluids with temperature-dependent viscosity: Application to the oceanic mantle: *Journal of Geophysical Research*, v. 99, p. 19,853–19,866, doi:10.1029/94JB01405.
- Davies, G.F., 1995, Punctuated tectonic evolution of the Earth: *Earth and Planetary Science Letters*, v. 136, no. 3, p. 363–379, doi:10.1016/0012-821X(95)00167-B.
- De Franco, R., Govers, R., and Wortel, M.J.R., 2006, Numerical comparison of different convergent plate contacts: Subduction channel and subduction fault: *Geophysical Journal International*, v. 171, no. 1, p. 435–450, doi:10.1111/j.1365-246X.2006.03498.x.
- Di Giuseppe, E., Van Hunen, J., Funiello, F., Faccenna, C., and Giardini, D., 2008, Slab stiffness control of trench motion: Insights from numerical models: *Geochemistry, Geophysics, Geosystems*, v. 9, Q02014, doi:10.1029/2007GC001776.
- Domeier, M.P., Doubrovine, V., Torsvik, T.H., Spakman, W., and Bull, A.L., 2016, Global correlation of lower mantle structure and past subduction: *Geophysical Research Letters*, v. 43, p. 4945–4953, doi:10.1002/2016GL068827.
- Elsasser, W.M., 1969, Convection and stress propagation in the upper mantle, in Runcorn, S.K., ed., *The Application of Modern Physics to the Earth and Planetary Interiors*: New York, John Wiley, p. 223–249.
- Faccenna, M., and Dal Zilio, L., 2017, The role of solid-solid phase transitions in mantle convection: *Lithos*, v. 268–271, p. 198–224, doi:10.1016/j.lithos.2016.11.007.

- Faccenna, C., Becker, T.W., Lucente, F.P., Jolivet, L., and Rossetti, F., 2001, History of subduction and back-arc extension in the Central Mediterranean: *Geophysical Journal International*, v. 145, p. 809–820, doi:10.1046/j.0956-540x.2001.01435.x.
- Faccenna, C., Heuret, A., Funicello, F., Lallemand, S., and Becker, T., 2007, Predicting trench and plate motion from the dynamics of a strong slab: *Earth and Planetary Science Letters*, v. 257, p. 29–36, doi:10.1016/j.epsl.2007.02.016.
- Faccenna, C., Becker, T.W., Conrad, C.P., and Husson, L., 2013, Mountain building and mantle dynamics: *Tectonics*, v. 32, p. 80–93, doi:10.1029/2012TC003176.
- Farrington, R.J., Moresi, L.N., and Capitanio, F.A., 2014, The role of viscoelasticity in subducting plates: *Geochemistry, Geophysics, Geosystems*, v. 15, p. 4291–4304, doi:10.1002/2014GC005507.
- Fei, Y., Van Orman, J., Li, J., Van Westrenen, W., Sanloup, C., Minarik, W., Hirose, K., Komyayashi, T., Walter, M., and Funakoshi, K., 2004, Experimentally determined postspinel transformation boundary in Mg₂SiO₄ using MgO as an internal pressure standard and its geophysical implications: *Journal of Geophysical Research*, v. 109, 2305, doi:10.1029/2003JB002562.
- Fischer, K.M., and Jordan, T.H., 1991, Seismic strain rate and deep slab deformation in Tonga: *Journal of Geophysical Research*, v. 96, no. B9, p. 14,429–14,444, doi:10.1029/91JB00153.
- Forsyth, D.W., 1975, Fault Plane Solutions and Tectonics of the South Atlantic and Scotia Sea: *Journal of Geophysical Research*, v. 80, no. 11, p. 1429–1443, doi:10.1029/JB080i011p01429.
- Forsyth, D.W., and Uyeda, S., 1975, On the relative importance of driving forces of plate motion: *Geophysical Journal of the Royal Astronomical Society*, v. 43, p. 163–200, doi:10.1111/j.1365-246X.1975.tb00631.x.
- Fourel, L., Goes, S., and Morra, G., 2014, The role of elasticity in slab bending: *Geochemistry, Geophysics, Geosystems*, v. 15, p. 4507–4525, doi:10.1002/2014GC005535.
- French, S.W., and Romanowicz, B.A., 2014, Whole-mantle radially anisotropic shear velocity structure from spectral-element waveform tomography: *Geophysical Journal International*, v. 199, no. 3, p. 1303–1327, doi:10.1093/gji/fgu334.
- Fukao, Y., and Obayashi, M., 2013, Subducted slabs stagnant above, penetrating through, and trapped below the 660 km discontinuity: *Journal of Geophysical Research*, v. 118, p. 5920–5938, doi:10.1002/2013JB010466.
- Fukao, Y., Obayashi, M., Inoue, H., and Nishii, M., 1992, Subducting slabs stagnant in the mantle transition zone: *Journal of Geophysical Research*, v. 97, p. 4809–4822, doi:10.1029/91JB02749.
- Fukao, Y., Widiyantoro, S., and Obayashi, M., 2001, Stagnant slabs in the upper and lower mantle transition zone: *Reviews of Geophysics*, v. 39, no. 3, p. 291–323, doi:10.1029/1999RG000068.
- Fukao, Y., Obayashi, M., Nakakuki, T., and the Deep Slab Project Group, 2009, Stagnant slab: A review: *Annual Review of Earth and Planetary Sciences*, v. 37, p. 19–46, doi:10.1146/annurev.earth.36.031207.124224.
- Funicello, F., Faccenna, C., Giardini, D., and Regenauer-Lieb, K., 2003a, Dynamics of retreating slabs: 2. Insights from three-dimensional laboratory experiments: *Journal of Geophysical Research*, v. 108, no. B4, 2207, doi:10.1029/2001JB000896.
- Funicello, F., Morra, G., Regenauer-Lieb, K., and Giardini, D., 2003b, Dynamics of retreating slabs: 1. Insights from two-dimensional numerical experiments: *Journal of Geophysical Research*, v. 108, no. B4, 2206, doi:10.1029/2001JB000898.
- Funicello, F., Moroni, M., Piromallo, C., Faccenna, C., Cenedese, A., and Bui, H.A., 2006, Mapping mantle flow during retreating subduction: Laboratory models analyzed by feature tracking: *Journal of Geophysical Research*, v. 111, B03402, doi:10.1029/2005JB003792.
- Funicello, F., Faccenna, C., Heuret, A., Lallemand, S., Di Giuseppe, E., and Becker, T., 2008, Trench migration, net rotation, and slab-mantle coupling: *Earth and Planetary Science Letters*, v. 271, p. 233–240, doi:10.1016/j.epsl.2008.04.006.
- Gaherty, J.B., and Hager, B.H., 1994, Compositional vs. thermal buoyancy and the evolution of subducted lithosphere: *Geophysical Research Letters*, v. 21, no. 2, p. 141–144, doi:10.1029/93GL03466.
- Garel, F., Goes, S., Davies, D.R., Davies, J.H., Kramer, S.C., and Wilson, C.R., 2014, Interaction of subducted slabs with the mantle transition zone: A regime diagram from 2-D thermo-mechanical models with a mobile trench and an overriding plate: *Geochemistry, Geophysics, Geosystems*, v. 15, p. 1739–1765, doi:10.1002/2014GC005257.
- Garfunkel, Z., Anderson, C.A., and Schubert, G., 1986, Mantle circulation and the lateral migration of subducted slab: *Journal of Geophysical Research*, v. 91, no. B7, p. 7205–7223, doi:10.1029/JB091iB07p07205.
- Giardini, D., and Woodhouse, J.H., 1984, Deep seismicity and modes of deformation in Tonga subduction zone: *Nature*, v. 307, p. 505–509, doi:10.1038/307505a0.
- Goes, S., Capitanio, F.A., and Morra, G., 2008, Evidence for lower mantle slab penetration phases in plate motions: *Nature*, v. 451, p. 981–984, doi:10.1038/nature06691.
- Goes, S., Capitanio, F.A., Morra, G., Seton, M., and Giardini, D., 2011, Signatures of downgoing plate-buoyancy driven subduction in Cenozoic plate motions: *Physics of the Earth and Planetary Interiors*, v. 184, p. 1–13, doi:10.1016/j.pepi.2010.10.007.
- Goes, S.D.B., Fourel, L., and Morra, G., 2014, Trench advance by the subduction of buoyant features: Application to the Izu-Bonin-Marianas Arc: *American Geophysical Union, Fall Meeting*, abstract T51B-4629.
- Gorbatov, A., and Fukao, Y., 2005, Tomographic search for missing link between the ancient Farallon subduction and the present Cocos subduction: *Geophysical Journal International*, v. 160, p. 849–854, doi:10.1111/j.1365-246X.2005.02507.x.
- Gorbatov, A., Kostoglodov, V., and Suárez, G., 1997, Seismicity and structure of the Kamchatka subduction zone: *Journal of Geophysical Research*, v. 102, no. B8, p. 17,883–888, doi:10.1029/96JB03491.
- Gorbatov, A., Widiyantoro, S., Fukao, Y., and Gordeev, E., 2000, Signature of remnant slabs in the North Pacific from P-wave tomography: *Geophysical Journal International*, v. 142, p. 27–36, doi:10.1046/j.1365-246x.2000.00122.x.
- Grand, S., van der Hilst, R.D., and Widiyantoro, S., 1997, Global seismic tomography: A snapshot of convection in the Earth: *GSA Today*, v. 7, p. 1–7.
- Grand, S.P., 1994, Mantle shear structure beneath the Americas and surrounding oceans: *Journal of Geophysical Research*, v. 99, p. 11,591–11,621, doi:10.1029/94JB00042.
- Grand, S.P., 2002, Mantle shear-wave tomography and the fate of subducted slabs: *Philosophical Transactions of the Royal Society of London. Series A: Mathematical and Physical Sciences*, v. 360, p. 2475–2491, doi:10.1098/rsta.2002.1077.
- Griffiths, R.W., Hackney, R.I., and van der Hilst, R.D., 1995, A laboratory investigation of effects of trench migration on the descent of subducted slabs: *Earth and Planetary Science Letters*, v. 133, no. 1–2, p. 1–17, doi:10.1016/0012-821X(95)00027-A.
- Guillou-Frottier, L., Buttles, J., and Olson, P., 1995, Laboratory experiments on the structure of subducted lithosphere: *Earth and Planetary Science Letters*, v. 133, no. 1–2, p. 19–34, doi:10.1016/0012-821X(95)00045-E.
- Gurnis, M., and Hager, B.H., 1988, Controls of the structure of subducted slabs: *Nature*, v. 335, p. 317–321, doi:10.1038/335317a0.
- Hafkenscheid, E., Buiter, S.J.H., Wortel, M.J.R., Spakman, W., and Bijwaard, H.M., 2001, Modelling the seismic velocity structure beneath Indonesia: A comparison with tomography: *Tectonophysics*, v. 333, p. 35–46, doi:10.1016/S0040-1951(00)00265-1.
- Hafkenscheid, E., Wortel, M.J.R., and Spakman, W., 2006, Subduction history of the Tethyan region derived from seismic tomography and tectonic reconstructions: *Journal of Geophysical Research*, v. 111, B08401, doi:10.1029/2005JB003791.
- Hager, B.H., 1984, Subducted slabs and the geoid: Constraints on mantle rheology and flow: *Journal of Geophysical Research*, v. 89, B7, p. 6003–6015, doi:10.1029/JB089iB07p06003.
- Hall, R., and Spakman, W., 2015, Mantle structure and tectonic history of SE Asia: *Tectonophysics*, v. 658, p. 14–45, doi:10.1016/j.tecto.2015.07.003.
- Han, L., and Gurnis, M., 1999, How valid are dynamic models of subduction and convection when plate motions are prescribed?: *Physics of the Earth and Planetary Interiors*, v. 110, p. 235–246, doi:10.1016/S0031-9201(98)00156-3.
- Hayes, G.P., Wald, D.J., and Johnson, R.L., 2012, Slab1.0: A three-dimensional model of global subduction zone geometries: *Journal of Geophysical Research*, v. 117, B01302, doi:10.1029/2011JB008524.
- Hirose, K., 2002, Phase transitions in pyrolytic mantle around 670-km depth: Implications for upwelling of plumes from the lower mantle: *Journal of Geophysical Research*, v. 107, 2078, doi:10.1029/2001JB000597.
- Hogrefe, A., Rubie, D.C., Sharp, T.G., and Seifert, F., 1994, Metastability of enstatite in deep subducting lithosphere: *Nature*, v. 372, no. 6504, p. 351–353, doi:10.1038/372351a0.
- Holland, T.J.B., Hudson, N.F.C., Powell, R., and Harte, B., 2013, New thermodynamic models and calculated phase equilibria in NCFMAS for basic and ultrabasic compositions through the transition zone into the uppermost lower mantle: *Journal of Petrology*, v. 54, no. 9, p. 1901–1920, doi:10.1093/petrology/egt035.
- Holt, A.F., Becker, T.W., and Buffett, B.A., 2015, Trench migration and overriding plate stress in dynamic subduction models: *Geophysical Journal International*, v. 201, p. 172–192, doi:10.1093/gji/ggv011.

- Holt, W.E., 1995, Flow fields within the Tonga Slab determined from moment tensors of deep earthquakes: *Geophysical Research Letters*, v. 22, no. 8, p. 989–992, doi:10.1029/95GL00786.
- Houseman, G.A., and Gubbins, D., 1997, Deformation of subducted oceanic lithosphere: *Geophysical Journal International*, v. 131, p. 535–551, doi:10.1111/j.1365-246X.1997.tb06598.x.
- Isacks, B., and Molnar, P., 1971, Distribution of stresses in the descending lithosphere from a global survey of focal mechanism solutions of mantle earthquakes: *Reviews of Geophysics*, v. 9, p. 103–174, doi:10.1029/RG009i001p00103.
- Ito, E., and Yamada, H., 1982, Stability relations of silicate spinels, ilmenites and perovskites, in Akimoto, S., and Maghni, M.H., eds., *High-Pressure Research in Geophysics: The Netherlands*, Springer, p. 405–419.
- Jagoutz, O., Royden, L., Holt, A.F., and Becker, T.W., 2015, Anomalously fast convergence of India and Eurasia caused by double subduction: *Nature Geoscience*, v. 8, no. 6, p. 475–478, doi:10.1038/ngeo2418.
- James, K.H., 2009, Evolution of Middle America and the in situ Caribbean Plate model, in James, K.H., Lorente, M.A., and Pindell, J.L., eds., *The Origin and Evolution of the Caribbean Plate: Geological Society of London Special Publication 328*, p. 127–138, doi:10.1144/SP328.4.
- Jarvis, G.T., and Lowman, J.P., 2007, Survival times of subducted slab remnants in numerical models of mantle flow: *Earth and Planetary Science Letters*, v. 260, p. 23–36, doi:10.1016/j.epsl.2007.05.009.
- Javoy, M., et al., 2010, The chemical composition of the Earth: Enstatite chondrite models: *Earth and Planetary Science Letters*, v. 293, p. 259–268, doi:10.1016/j.epsl.2010.02.033.
- Jolivet, L., and Faccenna, C., 2000, Mediterranean extension and the Africa-Eurasia collision: *Tectonophysics*, v. 19, p. 1095–1106, doi:10.1029/2000TC900018.
- Karason, H., and Van der Hilst, R.D., 2000, Constraints on mantle convection from seismic tomography, in Richards, M.A., Gordon, R.G., and Van Der Hilst, R.D., eds., *The History and Dynamics of Global Plate Motions: Washington, D.C., American Geophysical Union*, doi:10.1029/GM121p0277, p. 277–288.
- Karato, S.I., 1989, Plasticity—Crystal structure systematics in dense oxides and its implications for the creep strength of the Earth's deep interior: A preliminary result: *Physics of the Earth and Planetary Interiors*, v. 55, p. 234–240, doi:10.1016/0031-9201(89)90071-X.
- Karato, S.I., Riedel, M.R., and Yuen, D.A., 2001, Rheological structure and deformation of subducted slabs in the mantle transition zone: Implications for mantle circulation and deep earthquakes: *Physics of the Earth and Planetary Interiors*, v. 127, p. 83–108, doi:10.1016/S0031-9201(01)00223-0.
- Katsura, T., et al., 2004, Olivine-wadsleyite transition in the system (Mg,Fe)₂SiO₄: *Journal of Geophysical Research*, v. 109, B02209, doi:10.1029/2003JB002438.
- Khan, A., Connolly, J.A.D., and Taylor, S.R., 2008, Inversion of seismic and geodetic data for the major element chemistry and temperature of the Earth's mantle: *Journal of Geophysical Research*, v. 113, B09308, doi:10.1029/2007JB005239.
- Kincaid, C., and Olson, P., 1987, An experimental study of subduction and slab migration: *Journal of Geophysical Research*, v. 92, no. B13, p. 13,832–13,840.
- King, S.D., 2001, Subduction zones: Observations and geodynamic models: *Physics of the Earth and Planetary Interiors*, v. 127, p. 9–24, doi:10.1016/S0031-9201(01)00218-7.
- King, S.D., 2002, Geoid and topography over subduction zones: The effect of phase transformations: *Journal of Geophysical Research*, v. 107, p. ETG 2-1–ETP 2-10, doi:10.1029/2000JB000141.
- King, S.D., 2016, Reconciling laboratory and observational models of mantle rheology in geodynamic modelling: *Journal of Geodynamics*, v. 100, p. 33–50, doi:10.1016/j.jog.2016.03.005.
- King, S.D., and Hager, B.H., 1994, Subducted slabs and the geoid: 1. Numerical experiments with temperature-dependent viscosity: *Journal of Geophysical Research—Solid Earth*, v. 99, p. 19,843–19,852, doi:10.1029/94JB01552.
- King, S.D., and Ita, J., 1995, Effect of slab rheology on mass transport across a phase transition boundary: *Journal of Geophysical Research*, v. 100, p. 20,211–20,222, doi:10.1029/95JB01964.
- King, S.D., Frost, D.J., and Rubie, D.C., 2015, Why cold slabs stagnate in the transition zone: *Geology*, v. 43, p. 231–234, doi:10.1130/G36320.1.
- Kumar, P., Yuan, X., Kumar, M.R., Kind, R., Li, X., and Chadha, R.K., 2007, The rapid drift of the Indian tectonic plate: *Nature*, v. 449, p. 894–897, doi:10.1038/nature06214.
- Lallemand, S., Heuret, A., and Boutelier, D., 2005, On the relationships between slab dip, back-arc stress, upper plate absolute motion, and crustal nature in subduction zones: *Geochemistry, Geophysics, Geosystems*, v. 6, Q09006, doi:10.1029/2005GC000917.
- Lay, T., 1994, The fate of descending slabs: *Annual Review of Earth and Planetary Sciences*, v. 22, p. 33–61, doi:10.1146/annurev.ea.22.050194.000341.
- Lee, C., and King, S.D., 2011, Dynamic buckling of subducting slabs reconciles geological and geophysical observations: *Earth and Planetary Science Letters*, v. 312, p. 360–370, doi:10.1016/j.epsl.2011.10.033.
- Lee, T.Y., and Lawver, L.A., 1995, Cenozoic plate reconstruction of Southeast Asia: *Tectonophysics*, v. 251, p. 85–138, doi:10.1016/0040-1951(95)00023-2.
- Li, C., Van der Hilst, R.D., Engdahl, E.R., and Burdick, S., 2008, A new global model for *P* wave speed variations in Earth's mantle: *Geochemistry, Geophysics, Geosystems*, v. 9, Q05018, doi:10.1029/2007GC001806.
- Li, Z.-H., and Ribe, N.M., 2012, Dynamics of free subduction from 3-D boundary element modeling: *Journal of Geophysical Research*, v. 117, B06408, doi:10.1029/2012JB009165.
- Litasov, K., Ohtani, E., Sano, A., Suzuki, A., and Funakoshi, K., 2005, In situ X-ray diffraction study of postspinel transformation in a peridotite mantle: Implication for the 660-km discontinuity: *Earth and Planetary Science Letters*, v. 238, p. 311–328, doi:10.1016/j.epsl.2005.08.001.
- Loiselet, C., Husson, L., and Braun, J., 2009, From longitudinal slab curvature to slab rheology: *Geology*, v. 37, p. 747–750, doi:10.1130/G30052A.1.
- Loiselet, C., Braun, J., Husson, L., Le Carlier de Veslud, C., Thieulot, C., Yamato, P., and Grujic, D., 2010, Subducting slabs: Jellyfishes in the Earth's mantle: *Geochemistry, Geophysics, Geosystems*, v. 11, Q08016, doi:10.1029/2010GC003172.
- Lundgren, P., and Giardini, D., 1994, Isolated deep earthquakes and the fate of subduction in the mantle: *Journal of Geophysical Research*, v. 99, p. 15833–15842, doi:10.1029/94JB00038.
- Lyubetskaya, T., and Korenaga, J., 2007, Chemical composition of Earth's primitive mantle and its variance: 2. Implications for global geodynamics: *Journal of Geophysical Research*, v. 112, B03212, doi:10.1029/2005JB004224.
- Machetel, P., and Weber, P., 1991, Intermittent layered convection in a model with an endothermic phase change at 670 km: *Nature*, v. 350, p. 55–57, doi:10.1038/350055a0.
- Magni, V., van Hunen, J., Funiello, F., and Faccenna, C., 2012, Numerical models of slab migration in continental collision zones: *Solid Earth*, v. 3, p. 293–306, doi:10.5194/se-3-293-2012.
- Magni, V., Faccenna, C., van Hunen, J., and Funiello, F., 2014, How collision triggers backarc extension: Insight into Mediterranean style of extension from 3-D numerical models: *Geology*, v. 42, p. 511–514, doi:10.1130/G35446.1.
- Mallard, C., Coltice, N., Seton, M., Müller, R.D., and Tackley, P.J., 2016, Subduction controls the distribution and fragmentation of Earth's tectonic plates: *Nature*, v. 535, p. 140–143, doi:10.1038/nature17992.
- Marquardt, H., and Miyagi, L., 2015, Slab stagnation in the shallow lower mantle linked to an increase in mantle viscosity: *Nature Geoscience*, v. 8, p. 311–314, doi:10.1038/ngeo2393.
- Martinod, J., Funiello, F., Faccenna, C., Labanieh, S., and Regard, V., 2005, Dynamical effects of subducting ridges: Insights from 3-D laboratory models: *Geophysical Journal International*, v. 163, p. 1137–1150, doi:10.1111/j.1365-246X.2005.02797.x.
- Mason, W.G., Moresi, L., Betts, P.G., and Miller, M.S., 2010, Three-dimensional numerical models of the influence of a buoyant oceanic plateau on subduction zones: *Tectonophysics*, v. 483, p. 71–79, doi:10.1016/j.tecto.2009.08.021.
- McCrory, P.A., Blair, J.L., Waldhauser, F., and Oppenheimer, D.H., 2012, Juan de Fuca slab geometry and its relation to Wadati-Benioff zone seismicity: *Journal of Geophysical Research*, v. 117, B09306, doi:10.1029/2012JB009407.
- McDonough, W.F., and Sun, S.-s., 1995, The composition of the Earth: *Chemical Geology*, v. 120, p. 223–253, doi:10.1016/0009-2541(94)00140-4.
- McNamara, A.K., and Van Keken, P.E., 2000, Cooling of the Earth: A parameterized convection study of whole versus layered models: *Geochemistry, Geophysics, Geosystems*, v. 1, 1027, doi:10.1029/2000GC000045.
- Miller, M.S., Gorbатов, A., and Kennett, B.L.N., 2005, Heterogeneity within the subducting Pacific slab beneath the Izu-Bonin-Mariana arc: Evidence from tomography using 3D ray tracing inversion techniques: *Earth and Planetary Science Letters*, v. 235, p. 331–342, doi:10.1016/j.epsl.2005.04.007.
- Miller, M.S., Kennett, B.L.N., and Toy, V.G., 2006, Spatial and temporal evolution of the subducting Pacific plate structure along the western Pacific margin: *Journal of Geophysical Research*, v. 111, B02401, doi:10.1029/2005JB003705.
- Mitrovica, J.X., and Forte, A.M., 2004, A new inference of mantle viscosity based upon joint inversion of convection and glacial isostatic adjustment data: *Earth and Planetary Science Letters*, v. 225, p. 177–189, doi:10.1016/j.epsl.2004.06.005.

- Molnar, P., and Atwater, T., 1978, Interarc spreading and Cordilleran tectonics as alternates related to the age of subducted oceanic lithosphere: *Earth and Planetary Science Letters*, v. 41, p. 330–340, doi:10.1016/0012-821X(78)90187-5.
- Molnar, P., Freedman, D., and Shih, J.S.F., 1979, Lengths of intermediate and deep seismic zones and temperatures in downgoing slabs of lithosphere: *Geophysical Journal of the Royal Astronomical Society*, v. 56, p. 41–54, doi:10.1111/j.1365-246X.1979.tb04766.x.
- Moresi, L., and Gurnis, M., 1996, Constraints on the lateral strength of slabs from three-dimensional dynamic flow models: *Earth and Planetary Science Letters*, v. 138, p. 15–28, doi:10.1016/0012-821X(95)00221-W.
- Morra, G., and Regenauer-Lieb, K., 2006, A coupled solid-fluid method for modeling subduction: *Philosophical Magazine*, v. 86, no. 21–22, p. 3307–3323, doi:10.1080/14786430500256359.
- Morra, G., Regenauer-Lieb, K., and Giardini, D., 2006, On the curvature of oceanic arcs: *Geology*, v. 34, p. 877–880, doi:10.1130/G22462.1.
- Motoki, M.H., and Ballmer, M.D., 2015, Intraplate volcanism due to convective instability of stagnant slabs in the mantle transition zone: *Geochemistry, Geophysics, Geosystems*, v. 16, p. 538–551, doi:10.1002/2014GC005608.
- Müller, R.D., Sdrolias, M., Gaina, C., and Roest, W.R., 2008, Age, spreading rates and spreading asymmetry of the world's ocean crust: *Geochemistry, Geophysics, Geosystems*, v. 9, Q04006, doi:10.1029/2007GC001743.
- Myhill, R., 2012, Slab buckling and its effect on the distributions and focal mechanisms of deep-focus earthquakes: *Geophysical Journal International*, v. 192, p. 837–853, doi:10.1093/gji/ggs054.
- Nakakuki, T., Tagawa, M., and Iwase, Y., 2010, Dynamical mechanisms controlling formation and avalanche of a stagnant slab: *Physics of the Earth and Planetary Interiors*, v. 183, p. 309–320, doi:10.1016/j.pepi.2010.02.003.
- Nerlich, R., Colli, L., Ghelichkhan, S., Schubert, B., and Bunge, H.-P., 2016, Constraining central Neo-Tethys Ocean reconstructions with mantle convection models: *Geophysical Research Letters*, v. 43, p. 9595–9603, doi:10.1002/2016GL070524.
- Nishi, M., Kato, T., Kubo, T., and Kikigawa, T., 2008, Survival of pyropic garnet in subducting plates: *Physics of the Earth and Planetary Interiors*, v. 170, no. 3, p. 264–280, doi:10.1016/j.pepi.2008.03.013.
- Olbertz, D., Wortel, M.J.R., and Hansen, U., 1997, Trench migration and subduction zone geometry: *Geophysical Research Letters*, v. 24, p. 221–224, doi:10.1029/96GL03971.
- Panaszyuk, S.V., and Hager, B.H., 2000, Inversion for mantle viscosity profiles constrained by dynamic topography and the geoid, and their estimated errors: *Geophysical Journal International*, v. 143, p. 821–836, doi:10.1046/j.0956-540X.2000.01286.x.
- Papazachos, B.C., Karakostas, V.G., Papazachos, C.B., and Scordilis, E.M., 2000, The geometry of the Wadati-Benioff zone and lithospheric kinematics in the Hellenic Arc: *Tectonophysics*, v. 319, p. 275–300, doi:10.1016/S0040-1951(99)00299-1.
- Piromallo, C., and Morelli, A., 2003, P wave tomography of the mantle under the Alpine-Mediterranean area: *Journal of Geophysical Research*, v. 108, 2065, doi:10.1029/2002JB001757.
- Pysklywec, R.N., and Ishii, M., 2005, Time dependent subduction dynamics driven by the instability of stagnant slabs in the transition zone: *Physics of the Earth and Planetary Interiors*, v. 149, p. 115–132, doi:10.1016/j.pepi.2004.08.019.
- Pysklywec, R.N., Mitrovica, J.X., and Ishii, M., 2003, Mantle avalanche as a driving force for tectonic reorganization in the southwest Pacific: *Earth and Planetary Science Letters*, v. 209, p. 29–38, doi:10.1016/S0012-821X(03)00073-6.
- Ranalli, G., 1995, *Rheology of the Earth* (second edition): Netherlands, Springer, 414 p.
- Ren, Y., Stutzmann, E., Van der Hilst, R.D., and Besse, J., 2007, Understanding seismic heterogeneities in the lower mantle beneath the Americas from seismic tomography and plate tectonic history: *Journal of Geophysical Research*, v. 112, B01302, doi:10.1029/2005JB004154.
- Replumaz, A., Káráson, H., Van der Hilst, R.D., Besse, J., and Taponnier, P., 2004, 4-D evolution of SE Asia's mantle from geological reconstructions and seismic tomography: *Earth and Planetary Science Letters*, v. 221, p. 103–115, doi:10.1016/S0012-821X(04)00070-6.
- Ribe, N.M., 2010, Bending mechanics and mode selection in free subduction: A thin-sheet analysis: *Geophysical Journal International*, v. 180, p. 559–576, doi:10.1111/j.1365-246X.2009.04460.x.
- Ribe, N.M., Stutzmann, E., Ren, Y., and Van der Hilst, R.D., 2007, Buckling instabilities of subducted lithosphere beneath the transition zone: *Earth and Planetary Science Letters*, v. 254, p. 173–179, doi:10.1016/j.epsl.2006.11.028.
- Ricard, Y., Richards, M.A., Lithgow-Bertelloni, C., and Lestunff, Y., 1993, Geodynamic model of mantle density heterogeneity: *Journal of Geophysical Research*, v. 98, p. 21,895–21,909, doi:10.1029/93JB02216.
- Richards, M., and Engebretson, D.C., 1992, Large-scale mantle convection and the history of subduction: *Nature*, v. 355, p. 437–440, doi:10.1038/355437a0.
- Richter, F.M., 1973, Dynamical models for sea floor spreading: *Reviews of Geophysics and Space Physics*, v. 11, no. 2, p. 223–287, doi:10.1029/RG011i002p00223.
- Richter, F.M., 1979, Focal mechanisms and seismic energy release of deep and intermediate earthquakes in the Tonga-Kermadec Region and their bearing on the depth extent of mantle flow: *Journal of Geophysical Research*, v. 84, p. 6783–6795, doi:10.1029/JB084iB12p06783.
- Ringwood, A.E., 1975, *Composition and Petrology of the Earth's Mantle*: New York, McGraw-Hill, 618 p.
- Ross, M.I., and Scotese, C.R., 1988, A hierarchical tectonic model of the Gulf of Mexico and Caribbean region: *Tectonophysics*, v. 155, p. 139–168, doi:10.1016/0040-1951(88)90263-6.
- Schellart, W.P., 2008, Kinematics and flow patterns in deep mantle and upper mantle subduction models: Influence of the mantle depth and slab to mantle viscosity ratio: *Geochemistry, Geophysics, Geosystems*, v. 9, Q03014, doi:10.1029/2007GC001656.
- Schellart, W.P., and Spakman, W., 2012, Mantle constraints on the plate tectonic evolution of the Tonga-Kermadec-Hikurangi subduction zone and the South Fiji Basin: *Australian Journal of Earth Sciences*, v. 59, p. 933–952, doi:10.1080/08120099.2012.679692.
- Schellart, W.P., Jessell, M.W., and Lister, G.S., 2003, Asymmetric deformation in the backarc region of the Kuril arc, northwest Pacific: New insights from analogue modeling: *Tectonics*, v. 22, no. 5, 1047, doi:10.1029/2002TC001473.
- Schellart, W.P., Freeman, J., Stegman, D.R., Moresi, L., and May, D., 2007, Evolution and diversity of subduction zones controlled by slab width: *Nature*, v. 446, p. 308–311, doi:10.1038/nature05615.
- Schellart, W.P., Stegman, D.R., and Freeman, J., 2008, Global trench migration velocities and slab migration induced upper mantle volume fluxes: Constraints to find an Earth reference frame based on minimizing viscous dissipation: *Earth-Science Reviews*, v. 88, p. 118–144, doi:10.1016/j.earscirev.2008.01.005.
- Schmeling, H., Monz, R., and Rubie, D.C., 1999, The influence of olivine metastability on the dynamics of subduction: *Earth and Planetary Science Letters*, v. 165, no. 1, p. 55–66, doi:10.1016/S0012-821X(98)00249-0.
- Schmid, C., Goes, S., Van der Lee, S., and Giardini, D., 2002, Fate of the Cenozoic Farallon slab from a comparison of kinematic thermal modeling with tomographic images: *Earth and Planetary Science Letters*, v. 204, no. 1–2, p. 17–32, doi:10.1016/S0012-821X(02)00985-8.
- Sdrolias, M., and Müller, R.D., 2006, Controls on back-arc basin formation: *Geochemistry, Geophysics, Geosystems*, v. 7, Q04016, doi:10.1029/2005GC001090.
- Sigloch, K., 2011, Mantle provinces under North America from multifrequency *P* wave tomography: *Geochemistry, Geophysics, Geosystems*, v. 12, Q02W08, doi:10.1029/2010GC003421.
- Sigloch, K., and Mihalynuk, M.G., 2013, Intra-oceanic subduction shaped the assembly of Cordilleran North America: *Nature*, v. 496, p. 50–56, doi:10.1038/nature12019.
- Silver, P., Carlson, R.W., and Olson, P., 1988, Deep slabs, geochemical heterogeneity, and the large-scale structure of mantle convection: Investigation of an enduring paradox: *Annual Review of Earth and Planetary Sciences*, v. 16, p. 477–541, doi:10.1146/annurev.ea.16.050188.002401.
- Simmons, N.A., Myers, S.C., Johannesson, G., and Matzel, E., 2012, LLNL-G3Dv3: Global *P* wave tomography model for improved regional and teleseismic travel time prediction: *Journal of Geophysical Research*, v. 117, B10302, doi:10.1029/2012JB009525.
- Solheim, L.P., and Peltier, W.R., 1994, 660 km phase boundary deflections and episodically layered isochemical convection: *Journal of Geophysical Research*, v. 99, p. 15,861–15,875, doi:10.1029/94JB00730.
- Spakman, W., Van der Lee, S., and Van der Hilst, R.D., 1993, Travel-time tomography of the European-Mediterranean mantle down to 1400 km: *Physics of the Earth and Planetary Interiors*, v. 79, p. 3–74, doi:10.1016/0031-9201(93)90142-V.
- Stegman, D.R., Schellart, W.P., and Freeman, J., 2010a, Competing influences of plate width and far-field boundary conditions on trench migration and morphology of subducted slabs in the upper mantle: *Tectonophysics*, v. 483, p. 46–57, doi:10.1016/j.tecto.2009.08.026.
- Stegman, D.R., Farrington, R., Capitanio, F.A., and Schellart, W.P., 2010b, A regime diagram for subduction styles from 3-D numerical models of free subduction: *Tectonophysics*, v. 483, p. 29–45, doi:10.1016/j.tecto.2009.08.041.
- Stein, C.A., and Stein, S., 1992, A model for the global variation in oceanic depth and heat flow with lithospheric age: *Nature*, v. 359, p. 123–129, doi:10.1038/359123a0.
- Stein, S., Engeln, J.F., and Wiens, D.A., 1982, Subduction seismicity and tectonics in the lesser Antilles Arc: *Journal of Geophysical Research*, v. 87, p. 8642–8664, doi:10.1029/JB087iB10p08642.

- Stixrude, L., and Lithgow-Bertelloni, C., 2011, Thermodynamics of mantle minerals—II. Phase equilibria: *Geophysical Journal International*, v. 184, p. 1180–1213, doi:10.1111/j.1365-246X.2010.04890.x.
- Stixrude, L., Hemley, R.J., Fei, Y., and Mao, H.K., 1992, Thermoelasticity of silicate perovskite and magnesowüstite and stratification of the Earth's mantle: *Science*, v. 257, p. 1099–1101, doi:10.1126/science.2575073.1099.
- Tackley, P.J., Stevenson, D.J., Glatzmaier, G.A., and Schubert, S., 1993, Effects of an endothermic phase transition at 670 km depth in a spherical model of convection in the Earth's mantle: *Nature*, v. 361, p. 699–704, doi:10.1038/361699a0.
- Tackley, P.J., Xie, S., Nakagawa, T., and Hernlund, J.W., 2005, Numerical and laboratory studies of mantle convection: Philosophy, accomplishments and thermo-chemical structure and evolution, in Van der Hilst, R., Bass, J.D., Matas, J., and Trampert, J., eds., *Earth's Deep Mantle: Structure, Composition and Evolution*: Washington, D.C., American Geophysical Union, p. 83–99, doi:10.1029/160GM07.
- Tagawa, M., Nakakuki, T., and Tajima, F., 2007, Dynamical modeling of trench retreat driven by the slab interaction with the mantle transition zone: *Earth, Planets, and Space*, v. 59, p. 65–74, doi:10.1186/BF03352678.
- Tajima, F., and Grand, S.P., 1998, Variation of transition zone high-velocity anomalies and depression of 660 km discontinuity associated with subduction zones from the southern Kuriles to Izu-Bonin and Ryukyu: *Journal of Geophysical Research*, v. 103, p. 15,015–15,036, doi:10.1029/98JB00752.
- Tetzlaff, M., and Schmeling, H., 2009, Time-dependent interaction between subduction dynamics and phase transition kinetics: *Geophysical Journal International*, v. 178, no. 2, p. 826–844, doi:10.1111/j.1365-246X.2009.04182.x.
- Torii, Y., and Yoshioka, S., 2007, Physical conditions producing slab stagnation: Constraints of the Clapeyron slope, mantle viscosity, trench retreat, and dip angles: *Tectonophysics*, v. 445, p. 200–209, doi:10.1016/j.tecto.2007.08.003.
- Tosi, N., Čadež, O., and Martinec, Z., 2009, Subducted slabs and lateral viscosity variations: Effects on the long-wavelength geoid: *Geophysical Journal International*, v. 179, no. 2, p. 813–826, doi:10.1111/j.1365-246X.2009.04335.x.
- Turcotte, D.L., and Schubert, G., 1982, *Geodynamics: Applications of Continuum Physics to Geological Problems*: New York, John Wiley and Sons, 450 p.
- Van der Hilst, R.D., 1989, Importance of the reference model in linearized tomography and images of subduction below the Caribbean plate: *Geophysical Research Letters*, v. 16, no. 10, p. 1093–1096, doi:10.1029/GL016i010p01093.
- Van der Hilst, R.D., 1995, Complex morphology of subducted lithosphere in the mantle beneath the Tonga trench: *Nature*, v. 374, p. 154–157, doi:10.1038/374154a0.
- Van der Hilst, R.D., and Seno, T., 1993, Effects of relative plate motion on the deep structure and penetration depth of slabs below the Izu-Bonin and Mariana island arcs: *Earth and Planetary Science Letters*, v. 120, p. 395–407, doi:10.1016/0012-821X(93)90253-6.
- Van der Hilst, R.D., Engdahl, E.R., Spakman, W., and Nolet, G., 1991, Tomographic imaging of subducted lithosphere below northwest Pacific island arcs: *Nature*, v. 353, p. 37–43, doi:10.1038/353037a0.
- Van der Hilst, R.D., Widiyantoro, S., and Engdahl, E.R., 1997, Evidence for deep mantle circulation from global tomography: *Nature*, v. 386, p. 578–584, doi:10.1038/386578a0.
- Van der Lee, S., and Nolet, G., 1997, Upper mantle *S*-velocity structure of North America: *Journal of Geophysical Research*, v. 102, p. 22,815–22,838, doi:10.1029/97JB01168.
- Van der Meer, D.G., Spakman, W., Van Hinsbergen, D.J.J., Amaru, M.L., and Torsvik, T., 2009, Towards absolute plate motions constrained by lower-mantle slab remnants: *Nature Geoscience*, v. 3, p. 36–40, doi:10.1038/ngeo708.
- Van der Voo, R., Spakman, W., and Bijwaard, H., 1999a, Mesozoic subducted slabs under Siberia: *Nature*, v. 397, p. 246–249, doi:10.1038/16686.
- Van der Voo, R., Spakman, W., and Bijwaard, H., 1999b, Tethyan subducted slabs under India: *Earth and Planetary Science Letters*, v. 171, p. 7–20, doi:10.1016/S0012-821X(99)00131-4.
- Van Dinther, Y., Morra, G., Funicello, F., and Faccenna, C., 2010, Role of the overriding plate in the subduction process: Insights from numerical models: *Tectonophysics*, v. 484, no. 1–4, p. 74–86, doi:10.1016/j.tecto.2009.08.038.
- van Hinsbergen, D.J., Steinberger, B., Doubrovine, P., and Gassmöller, R., 2011, Acceleration-deceleration cycles of India-Asia convergence: Roles of mantle plumes and continental collision: *Journal of Geophysical Research*, v. 116, B06101, doi:10.1029/2010JB008051.
- Van Hunen, J., Van den Berg, A., and Vlaar, N.J., 2002, The impact of the South-American plate motion and the Nazca Ridge subduction on the flat subduction below South Peru: *Geophysical Research Letters*, v. 29, 1690, doi:10.1029/2001GL014004.
- Van Keken, P.E., and Zhong, S., 1999, Mixing in a 3D spherical model of present-day mantle convection: *Earth and Planetary Science Letters*, v. 171, no. 4, p. 533–547, doi:10.1016/S0012-821X(99)00181-8.
- Van Mierlo, W.L., Langenhorst, F., Frost, D.J., and Rubie, D.C., 2013, Stagnation of subducting slabs in the transition zone due to slow diffusion in majoritic garnet: *Nature Geoscience*, v. 6, no. 5, p. 400–403, doi:10.1038/ngeo1772.
- Vassiliou, M.S., and Hager, B.H., 1988, Subduction zone earthquakes and stress in slabs: *Pure and Applied Geophysics*, v. 128, no. 3/4, p. 547–624, doi:10.1007/BF00874550.
- Williams, S., Flament, N., Müller, R.D., and Butterworth, N.P., 2015, Absolute plate motions since 130 Ma constrained by subduction zone kinematics: *Earth and Planetary Science Letters*, v. 418, p. 66–77, doi:10.1016/j.epsl.2015.02.026.
- Wortel, M.J.R., 1982, Seismicity and rheology of subducted slabs: *Nature*, v. 296, p. 553–556, doi:10.1038/296553a0.
- Wortel, M.J.R., and Spakman, W., 2000, Subduction and slab detachment in the Mediterranean-Carpathian Region: *Science*, v. 290, no. 5498, p. 1910–1917.
- Xu, W., Lithgow-Bertelloni, C., Stixrude, L., and Ritsema, J., 2008, The effect of bulk composition and temperature on mantle seismic structure: *Earth and Planetary Science Letters*, v. 275, no. 1–2, p. 70–79, doi:10.1016/j.epsl.2008.08.012.
- Yamazaki, D., and Karato, S.I., 2001, Some mineral physics constraints on the rheology and geothermal structure of Earth's lower mantle: *The American Mineralogist*, v. 86, p. 385–391, doi:10.2138/am-2001-0401.
- Yanagisawa, T., Yamagishi, Y., Hamano, Y., and Stegman, D.R., 2010, Mechanism for generating stagnant slabs in 3-D spherical mantle convection models at Earth-like conditions: *Physics of the Earth and Planetary Interiors*, v. 183, p. 341–352, doi:10.1016/j.pepi.2010.02.005.
- Zahirovic, S., Müller, R.D., Seton, M., and Flament, N., 2015, Tectonic speed limits from plate kinematic reconstructions: *Earth and Planetary Science Letters*, v. 418, p. 40–52, doi:10.1016/j.epsl.2015.02.037.
- Zhong, S., and Davies, G.F., 1999, Effects of plate and slab viscosities on the geoid: *Earth and Planetary Science Letters*, v. 170, p. 487–496, doi:10.1016/S0012-821X(99)00124-7.
- Zhong, S., and Gurnis, M., 1994, Role of plates and temperature-dependent viscosity in phase change dynamics: *Journal of Geophysical Research*, v. 99, p. 15,903–917, doi:10.1029/94JB00545.
- Zhong, S., and Gurnis, M., 1995, Mantle convection with plates and mobile, faulted plate margins: *Science*, v. 267, p. 838–843, doi:10.1126/science.267.5199.838.
- Zhong, S., and Gurnis, M., 1997, Dynamic interaction between tectonic plates, subducting slabs, and the mantle: *Earth Interactions*, v. 1, no. 3, 18 p., doi:10.1175/1087-3562(1997)001<0001:DIBTPS>2.3.CO;2.
- Zhou, H.-W., and Clayton, R.W., 1990, P and S wave travel time inversions for subducting slab under the island arcs of the northwest Pacific: *Journal of Geophysical Research*, v. 95, no. B5, p. 6829–6851, doi:10.1029/JB095iB05p06829.